Ecological Monographs, 84(1), 2014, pp. 69–90

Stochastic models reveal conditions for cyclic dominance in sockeye salmon populations

J. Wilson White,[1,2,4] Louis W. Botsford,[1] Alan Hastings,[3] and Matthew D. Holland[1,5]

[1]*Department of Wildlife, Fish, and Conservation Biology, University of California, One Shields Avenue, Davis, California 95616 USA*
[2]*Department of Biology and Marine Biology, University of North Carolina, 601 South College Road, Wilmington, North Carolina 28403 USA*
[3]*Department of Environmental Science and Policy, University of California, One Shields Avenue, Davis, California 95616 USA*

Abstract. The cause of population cycles is a common question in ecology, and one especially puzzling case is the cycles over the past century in populations of sockeye salmon, *Oncorhyncus nerka*. Some populations of this semelparous species in British Columbia, Canada, exhibit a phenomenon termed *cyclic dominance*: every four years there is a dominant cohort of primarily four-year-old spawners, orders of magnitude more abundant than other cohorts, producing a distinctive four-year cycle. In some populations, these cycles stop, start, or shift phase. We used a stochastic age-structured model to investigate the conditions allowing cycles and the events that could cause them to move in and out of cyclic dominance. We first defined cyclic dominance as high values of *cyclicity*, the fraction of time the population is cyclic, and *dominance*, the difference in abundance between the dominant cohort and the other three cohorts. We then used simulations to determine the values of (1) relative population persistence (i.e., proximity to collapse), (2) variability in survival, (3) variability in growth, and (4) spread in spawning age distribution that led to the observed levels of cyclic dominance in 18 stocks from the Fraser River, British Columbia, and nine stocks from Bristol Bay, Alaska, USA. Our simulations produced a range of dynamics similar to those observed in real stocks, from noncyclic to intermittent cycles to extremely consistent cyclic-dominant cycles. We found that cyclicity and dominance were most likely to be high under conditions of low population persistence, high variability in survival, and narrow age structure. Populations could be driven into cyclic-dominant behavior by unusually large perturbations in survival, but not in individual growth rate. Because this triggering mechanism is stochastic, populations may exist under conditions enabling cycles for a substantial time without displaying cyclic dominance, which is consistent with observations from real stocks. The association between cyclic dominance and low population persistence is of some concern for management. Also, the dependence of cyclic variability on intrinsic population dynamics (albeit stochastically driven) should be taken into account when assessing whether statistically independent fluctuations of stocks produce a biodiversity portfolio effect.

Key words: Bristol Bay, Alaska, USA; cohort resonance; cyclic dominance; environmental stochasticity; Fraser River, British Columbia, Canada; Oncorhyncus nerka; *population cycles; population dynamics; portfolio effect; sockeye salmon.*

Introduction

Periodic fluctuations in abundance are a striking feature of the population dynamics of many species, and identifying the mechanisms driving population cycles is a long-standing focus in ecology (Volterra 1927, May 1973, Murdoch 1994, Higgins et al. 1997, Turchin et al. 2003). Classic examples of cyclic behavior can be found in taxa ranging from herbivorous insects (Turchin et al. 2003) to terrestrial rodents (Hanski et al. 2001) and marine invertebrates (Botsford and Wickham 1978), and population models have been used to elucidate possible mechanisms for the cycles in each case. The need to understand the origin of cyclic behavior is especially pressing for commercially important species, because cyclic resources are difficult to manage and impose hardships on humans dependent on those populations.

Population cycles can be produced by a variety of factors, and it is often possible to deduce the underlying mechanism from the cyclic pattern itself. For example, populations that are coupled tightly to a single resource or predator species typically show low-frequency "consumer–resource" cycles with a period greater than four generation times (referred to as $4T$), whereas single-species systems with either direct or delayed density-dependent feedbacks exhibit cycles with shorter periods

Manuscript received 16 December 2012; revised 29 April 2013; accepted 23 July 2013. Corresponding Editor: J. D. Reeve.
[4] E-mail: whitejw@uncw.edu
[5] Present address: California Delta Stewardship Council, Delta Science Program, 980 9th St., Sacramento, California 95814 USA.

(Gurney et al. 1983, Murdoch et al. 2002, Turchin 2003). Because different cycle-generating mechanisms tend to produce characteristic dynamics (as measured by the period and persistence of the cycles), population models are an invaluable tool for diagnosing the source of cyclic behavior and determining whether proposed mechanisms can actually produce the observed dynamics (Turchin 2003). In some cases, cycles arise because a population is locally unstable about an equilibrium (i.e., a fixed point), and the dominant mode of the local system leads to nonlinear cyclic behavior. For example, overcompensatory (i.e., declining at high density) density-dependent recruitment can cause cycles of period $2T$ in age-structured deterministic models, as is observed in populations of Dungeness crab (*Cancer magister*; Botsford and Wickham 1978, Botsford 1997). The deterministic nature of this type of population dynamics allows investigations of causal mechanisms to rely on the fact that if population parameters satisfy the conditions required for cyclic behavior (e.g., the rate of cannibalism of adults on juveniles; Botsford and Wickham 1978), then the population should exhibit cycles. Deducing mechanisms is more difficult for populations in which dynamics are deterministically stable and cycles are driven by stochastic forcing. For example, in age-structured models without density dependence (e.g., Leslie matrices; Caswell 2001), a random perturbation to the number of births at one time will tend to "echo" when that cohort matures, perturbing the number of births a generation later (Sykes 1969, Taylor 1979). Even in populations with density-dependent recruitment that is not overcompensatory, this effect causes a phenomenon termed "cohort resonance," in which the presence of random forcing, even with white noise, keeps a population away from equilibrium, thus constantly displaying the transient behavior of cycles with period equal to T (Bjørnstad et al. 1999, 2004, Worden et al. 2010). Because cohort resonance is initiated by stochasticity, a population may possess the necessary conditions for the existence of cycles (e.g., particular parameter values), but not exhibit cycles because the environment has not yet "nudged" the system into cyclic behavior. This introduces difficulty into the investigation of cycle-generating mechanisms, because one can identify the set of conditions that allow cycles, but a natural population that meets those conditions may not be observed to cycle.

A well-known, extreme, and not completely understood example of cyclic population dynamics is found at some times in some, but not all, populations of sockeye salmon (*Oncorhyncus nerka*; see Plate 1) that spawn in the watershed of the Fraser River in British Columbia, Canada. Similar behavior is also observed in some sockeye salmon populations spawning in rivers that drain into Bristol Bay, Alaska, USA. Like other Pacific salmon species, sockeye salmon are anadromous and semelparous. In the Fraser river, spawning occurs in the summer and fall in gravel beds in streams. Offspring spend their first winter in the gravel as eggs or alevins (newly hatched salmon), followed by one year (sometimes two) spent in lakes near the spawning grounds. After their second winter, smolts travel to the ocean, where they spend two years, returning as adults to the spawning grounds four years after they were spawned, with some adults returning one year sooner and some one year later (Groot and Margolis 1991). In Bristol Bay, life histories are more variable, with a greater variety of combinations of time spent in freshwater and the ocean, and most fish return five years after spawning (Groot and Margolis 1991).

Because of the regular timing and minimal overlap of cohorts, the spawning stock in a given stream in the Fraser River has commonly been viewed as essentially consisting of four (five in Bristol Bay) dynamically independent "lines" (i.e., quasi-independent populations), each of which spawns once every four years (approximately five years in Bristol Bay). Many of these sockeye stocks exhibit consistent cycles with two key characteristics. First, the period is equal to the generation time, T ($T = 4$ years in Fraser River, 5 years in Bristol Bay). Second, there is a single "dominant" line that has an abundance at least one order of magnitude greater than the next most abundant line. There is often a second-most-abundant (or "subdominant") line with greater abundance than the two remaining lines. Time series of spawner abundance for several representative stocks are shown in Fig. 1. Some populations have exhibited regular cycles for decades (e.g., Late Shuswap and Quesnel; Fig. 1A, B), others have started and stopped cycling (e.g., Raft, Kvichak, and Stellako; Fig. 1C–E), while still others have not exhibited period T cycles since data collection began (e.g., Harrison and Alagnak; Fig. 1F, G). In the cyclic stocks, the phase of the cycles occasionally shifts (i.e., the identity of the dominant line [line 1, 2, 3, or 4, based on the dominant year of spawning] switches, as in Stellako; Fig. 1E), and cycles of different stocks are out of phase (e.g., Late Shuswap and Quesnel; Fig. 1A, B), suggesting that the factors influencing the cycles occur in the spawning grounds rather than in the ocean.

The Fraser River sockeye cycles have been known since at least the onset of industrial fishing for sockeye in the late 19th century (Ricker 1950). The factors driving these cycles are of considerable practical interest, as the sockeye fishery is both economically important and quite fragile, with declining abundances in recent years requiring fishery closures (Peterman et al. 2010), although the 2010 run was anomalously high (Peterman and Dorner 2011). Recent identification of the importance of the portfolio effect also raises interest in the nature of variability in sockeye stocks (e.g., Schindler et al. 2010). An improved understanding of the cyclic behavior may improve management of this species. Ricker (1950) was one of the first to propose explanatory mechanisms for the cycles, and, to date, a variety of explanations have been offered, including depensatory

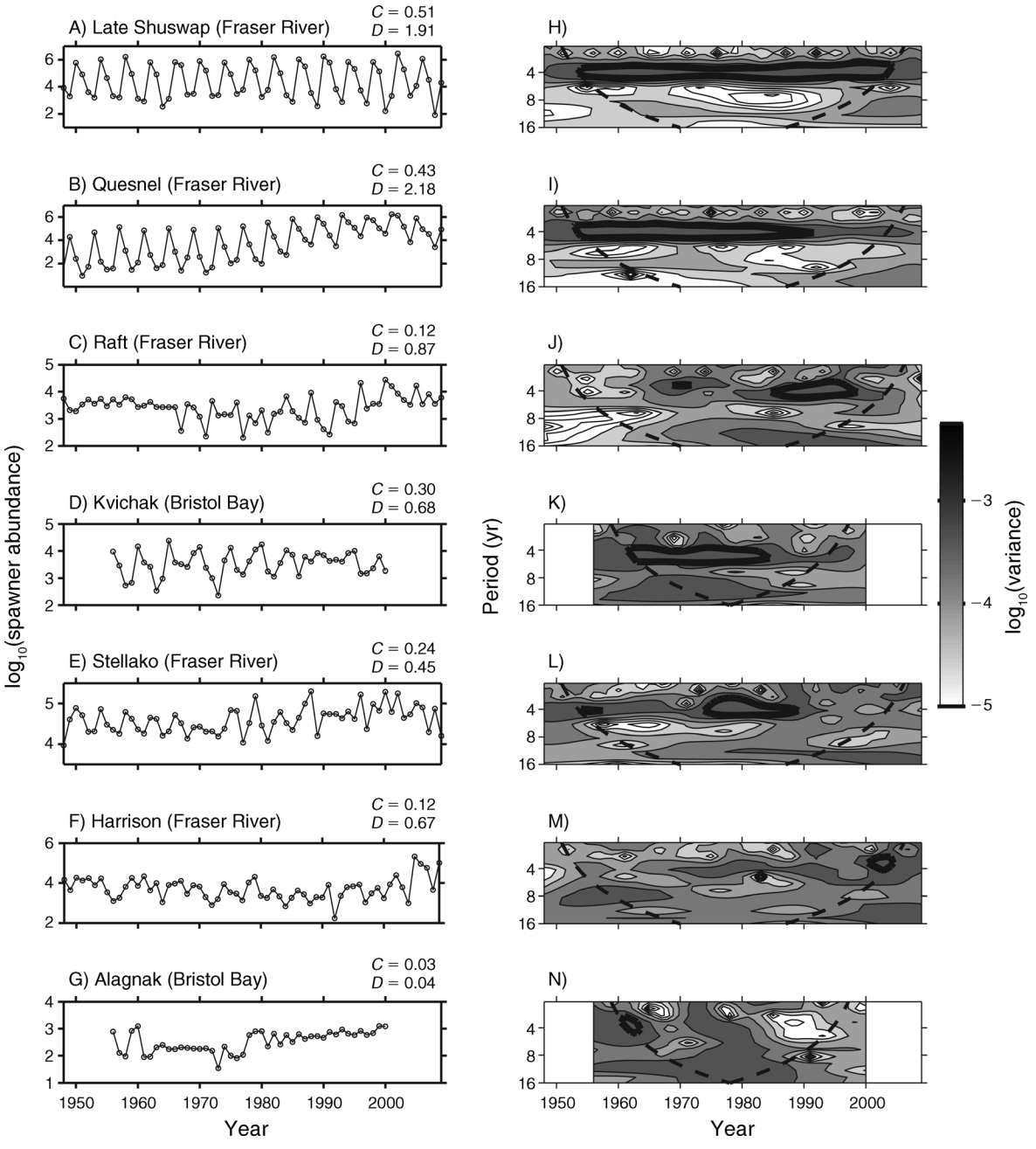

FIG. 1. (A–G) Representative time series and (H–N) wavelet spectra of sockeye salmon (*Oncorhyncus nerka*) stocks in the Fraser River (British Columbia, Canada) and Bristol Bay (Alaska, USA) regions. For each time series (A–G), the cyclic consistency (*C*) and dominance (*D*) were calculated from the wavelet spectra; *C* is a measure of how consistently the spectrum had high power at the dominant period (four years for Fraser River, five years for Bristol Bay), whereas *D* is a measure of how dominant one cycle-line was over the other cycle lines during periods of cycling at the dominant period. Shading in panels H–N indicates local variance of the time series at each period. Time series were normalized prior to wavelet analysis, so the variance scale is equivalent for all of the time series, despite large differences in actual abundance (note differing vertical axis scales in panels A–G). The dashed line in panels H–N indicates the cone of influence, outside of which edge effects distort the spectrum. The thick black contour encloses regions with variance significantly greater ($\alpha = 0.05$) than a red-noise process with the same lag-1 autocorrelation as the original time series. Power spectra were calculated using the Morlet mother wavelet (Torrence and Compo 1998).

harvesting (Walters and Staley 1987, Levy and Wood 1992, Ricker 1997), delayed density-dependent mortality (Ricker 1950, Larkin 1971), environmental variation in juvenile survival (Myers et al. 1998), heritability of spawning age and gene × environment interactions (Ricker 1972, reviewed by Ricker 1997), and consumer–resource interactions in spawning lakes (Ricker 1950, Guill et al. 2011, Schmitt et al. 2012). So far none of

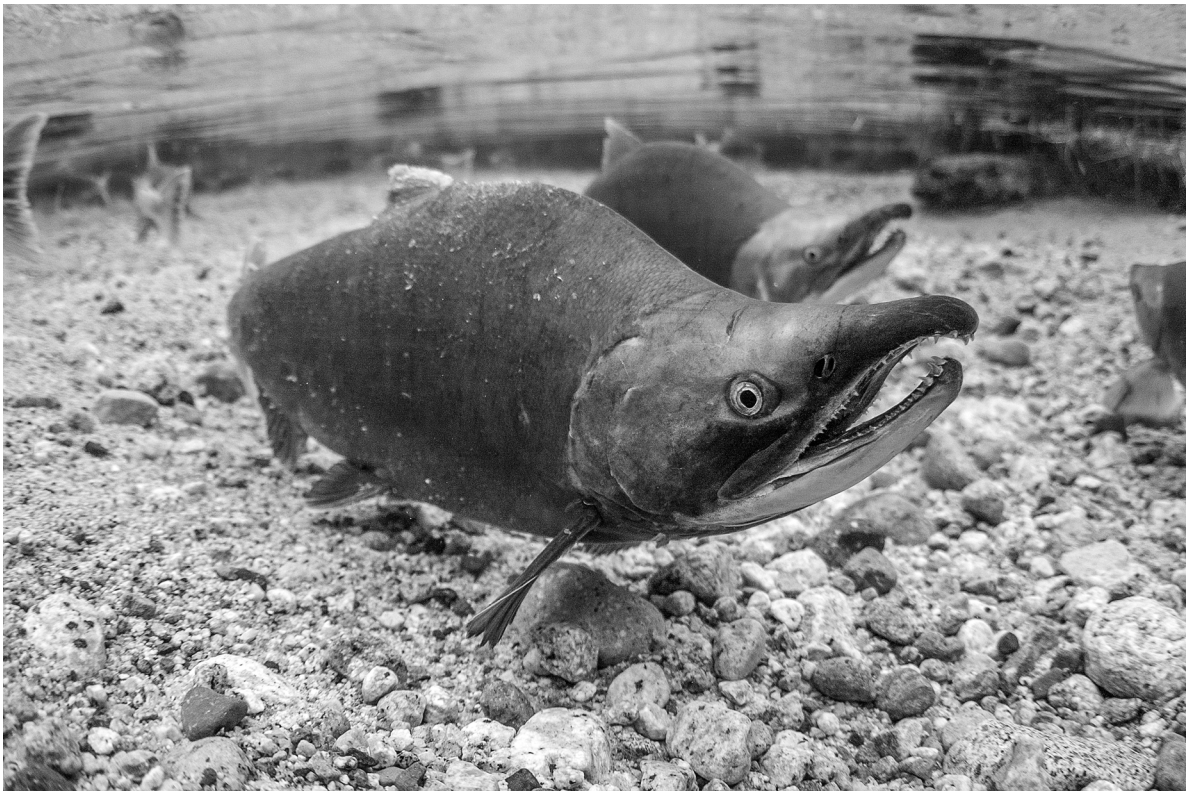

PLATE 1. Male sockeye salmon (*Oncorhyncus nerka*) on the spawning grounds at Knutson Creek, Lake Iliamna, Alaska, USA, August 2012. Fish spawning in Lake Iliamna are in the Kvichak stock. Photo credit: Morgan Bond.

these mechanisms has been able to satisfactorily recreate all of the unique features observed in sockeye time series, and evidence suggests that some of the proposed mechanisms (e.g., depensatory fishing) may not be present at all (Myers et al. 1998).

Myers et al. (1998) suggested that cohort resonance was sufficient to explain cycles in Fraser River sockeye stocks (although they did not refer to the phenomenon by that name), and that it was unnecessary to invoke more complicated population dynamics mechanisms such as depensatory harvest or delayed density dependence. They employed a relatively simple age-structured model of salmon population dynamics linearized about the equilibrium, and showed that small stochastic deviations (representing environmental forcing) in juvenile survival produced cycles with amplitude and frequency (period = $1T$) strikingly similar to those seen in the Fraser River. More recently, Worden et al. (2010) analyzed a similarly linearized, age-structured model to examine the effect of environmentally forced stochastic variation in both age-1 survivorship and individual growth rates of Pacific salmon and found that growth forcing actually produced a much stronger period-T response than did survival forcing. The effect of variable individual growth in this model was to vary the spawning age distribution between young and old ages. Both Myers et al. (1998) and Worden et al. (2010) noted that cycles were more likely to occur as fishing decreased adult survival and abundance, essentially because fishing pushes the population to the steeper ascending limb of the density-dependent stock–recruit curve, thus reducing density-dependent damping. However, neither model reproduced all of the distinctive features of cyclic dominance seen in some Fraser River stocks. In particular, Myers et al. (1998) did not explore the characteristics that could cause populations to shift between cyclic and noncyclic states, and did not evaluate the effects of variable growth rate.

Here we extend these earlier analyses to examine the interactions between parameter values and the nature of stochastic forcing (of both survival and age at spawning) that produce cyclic and noncyclic states. We first develop specific mathematical definitions of the two characteristics of these cycles: cyclicity and single-age-class dominance. We then examine the values of these characteristics for a number of sockeye salmon stocks from the Fraser River and Bristol Bay. We use an age-structured simulation model to determine ranges of parameter values that lead to specific combinations of the two characteristics of the "cyclic dominance" seen in sockeye salmon stocks. Importantly, our simulations reveal that strong cyclic dominance occurs only in simulations in which lifetime egg production is near the point of minimum required replacement, below which

TABLE 1. Parameter values used in simulations for sockeye salmon (*Oncorhyncus nerka*).

Parameter	Description	Range of values used
f	per capita fecundity†	4000 eggs per spawner
s_A	adult survivorship	0.6
$\bar{s}_J$	mean juvenile survivorship	0.34–0.6
$\bar{\mu}_p$	mean age at spawning‡	4 yr
α	Beverton-Holt initial slope§	0.0027
β	Beverton-Holt asymptote§	0.032 fish
σ_p	standard deviation of individual spawning age (spread of spawning age distribution)¶	0–0.45 yr
σ_s	coefficient of variation of juvenile survival (survival forcing)	0–1.5
σ_g	standard deviation of mean age at spawning (growth forcing)	0–0.3 yr

† Approximate average for Fraser River stocks (Gustafson et al. 1997).
‡ Value observed in all Fraser River stocks.
§ Mean of value estimated from nonlinear least-squares fit of Beverton-Holt curves to each Fraser River spawner–recruit data set.
¶ Values are in this range for 80% of Fraser River stocks.

collapse occurs (i.e., equilibrium recruitment is zero, Sissenwine and Shepherd 1987), a result with strong implications for fishery management.

METHODS

Model

We simulated sockeye salmon dynamics using a model with age structure and a density-dependent egg–recruitment relationship, similar to that used by Worden et al. (2010). This model has the form

$$\begin{bmatrix} x_1(t+1) \\ x_2(t+1) \\ x_3(t+1) \\ x_4(t+1) \\ x_5(t+1) \\ x_6(t+1) \end{bmatrix} = \begin{bmatrix} R[E(t)] \\ (1-p_1)s_J x_1(t) \\ (1-p_2)s_A x_2(t) \\ (1-p_3)s_A x_3(t) \\ (1-p_4)s_A x_4(t) \\ (1-p_5)s_A x_5(t) \end{bmatrix} \quad (1)$$

where $x_i(t)$ is the number of individuals in age class i at time t; $E(t) = \sum_{i=1}^{n} f p_i x_i(t)$ is the egg production at time t, which is a product of the age-specific probability of spawning given that an individual has not spawned yet (p_i) and fecundity (f), which we assume is essentially constant with age (Groot and Margolis 1991). The factors $(1 - p_i)$ represent mortality associated with death after spawning in this semelparous species. $R(E) = \alpha E/(1 + \beta E)$ is the Beverton-Holt egg–recruit relationship, s_J is the survival rate of juveniles in the first year of life, and s_A is the survival rate of older (adult) individuals (parameter values are given in Table 1). The Ricker stock–recruitment relationship is also commonly utilized for sockeye salmon (e.g., Myers et al. 1998). A visual comparison of fits of both stock–recruitment relationships to the data indicated that dynamic behavior would not differ qualitatively between the two, so we followed the examples of Barrowman et al. (2003) and Pyper et al. (2005) in using the Beverton-Holt relationship.

A cohort can experience stochastic variability in survival or growth. We specified stochasticity in survival (s_J) only in the first year of life. Because the abundance of fish in older age classes is a product of annual survivals to that age, the effects of temporal variability in s_J in our model are similar to the effects that we would obtain if we varied survival during the freshwater, ocean entry, or ocean stages, at any time prior to the onset of spawning in a cohort. We specified variability in growth in terms of its effect on the mean age at spawning of a cohort. We assumed that, in general, later spawning is due to slower growth and earlier spawning is due to faster growth. It is important to clarify that our analysis is concerned with the effects of variability in survival and variability in age at spawning, regardless of the sources of that variability. That is, our analysis does not address or depend on the particular mechanisms (or their timing) that lead to variability in survival or growth.

Because of the way in which we specify temporal variability in our model, the s_J and p_i parameters were specific to each cohort (the recruits spawned in a particular year), but were allowed to vary among cohorts. Abundance of salmon is estimated when they return to freshwater to spawn, so the "observed" abundance of spawners at time t is the sum of individuals from all cohorts that are spawning at t (from Eq. 1, up to six cohorts could be living at any time).

We assumed that survival in early life could vary due to environmental forcing and was log-normally distributed (Peterman 1981), so $s_J(t) = \exp(\xi(t))$, where $\xi(t)$ is a normally distributed, time-dependent forcing signal. This implies that the mean of $\xi(t)$ was $\log(\bar{s}_J)$, where $\bar{s}_J$ is the geometric mean of juvenile survival. We specified the coefficient of variation (CV) of $\xi(t)$ to be σ_s. We specified the CV of $\xi(t)$ rather than the variance so that simulations with different values of $\bar{s}_J$ would have similar variances of s_J (if the variance of $\xi(t)$ had been held constant, the variance of s_J would have increased with $\bar{s}_J$).

The probability that an individual in a cohort spawns at a given age i, p_i, was assumed to follow a cumulative normal distribution (z) of age a, with mean age at spawning of the cohort born in year t $\mu_p(t)$ and standard deviation about the mean size σ_p:

$$z\left(a-\mu_p(t)\right)=\frac{1}{\sigma_p\sqrt{2\pi}}\exp\left[-\frac{\left(a-\mu_p(t)\right)^2}{2\sigma_p^2}\right] \quad (2a)$$

$$p_i=\int_{-\infty}^{i+0.5} z\left(a-\mu_p(t)\right)da. \quad (2b)$$

Note that the integral in Eq. 2b is evaluated from $-\infty$ to $i + 0.5$; this is because we treat age as a continuous variable in Eq. 2, but spawning must occur at a single distinct time within the calendar year. Thus we integrate over ages (da) that are within one half-year of the mean spawning age. The model in Eq. 1 has up to six age classes, so it is able to represent dynamics for Bristol Bay populations, where the mean age of spawning is approximately 5 years, but some fish delay to age 6. If the mean age at spawning is 4 years with a small value of σ_p (as was the case for simulations that approximate the Fraser River populations; Table 1) $p_5 \approx 1$ and essentially no fish survive to enter the sixth age class.

We assumed that the probability of spawning depends on age, so we represented environmentally driven variability in growth as variability in the mean age at spawning: $\mu_p(t) = \zeta(t)$, where $\bar{\mu}_p$ is the overall mean age of spawning and $\zeta(t)$ is a time-dependent forcing signal with mean of $\bar{\mu}_p$ (the overall mean age of spawning) and standard deviation σ_g.

We simulated salmon population dynamics for a range of juvenile survival rates $\bar{s}_J$, spawning age distribution spread σ_p, and levels of environmental variability in both survival, σ_s, and growth, σ_g (Table 1). We held all other demographic parameters constant across simulations (Table 1). Thus our analysis focuses exclusively on the potential for differences in cyclic dynamics due to differences in environmental variability and productivity (which is determined in part by $\bar{s}_J$; see discussion of lifetime egg production in the next paragraph). We assume that among-stock differences in carrying capacity and other parameters do not contribute to differences in cyclic behavior.

For each combination of $\bar{s}_J$ and σ_p, we also calculated the lifetime egg production (LEP), the total expected number of eggs produced by a single individual in that cohort. This is equal to the sum of cumulative survival to each age, $l_i = s_J s_A^{(i-2)}$, times the egg production at that age: LEP $= \sum_{i=1}^{n} f p_i l_i$. A population will persist (i.e., have a nonzero deterministic equilibrium) only if αLEP > 1, where α is the slope at the origin of the egg–recruit relationship. When that inequality is satisfied, each adult replaces itself with at least one offspring in the next generation (Sissenwine and Shepherd 1987). We characterized the proximity of the population to deterministic collapse as "persistence," P, calculated as $P = \log_{10}(\alpha\text{LEP})$, that is, the logarithm of the ratio of LEP to the value required for replacement (i.e., for persistence).

Simulations were started from the deterministic equilibrium and run for 200 years, extracting the time series of spawner density in the final 50 years for comparison to empirical data sets of approximately the same length. We performed model simulations for a range in parameter values, focusing on those that affected LEP (Table 1); this yielded a total of 3024 distinct parameter combinations, and we performed 100 simulations for each parameter combination (MATLAB code used in model analysis is provided in the Supplement).

Data

We obtained time series of spawner abundance and recruit age distribution from approximately 1948 to 2009 for 19 Fraser River (British Columbia, Canada) sockeye stocks and nine Bristol Bay (Alaska, USA) stocks (Fig. 1; Appendix: Fig. A1). Data availability varied among stocks; the full 62-year range was available for most Fraser River stocks, and the shortest time series was 22 years (Nushagak, Bristol Bay). "Recruits" in this data set are adults returning to freshwater to spawn, and they are enumerated prior to the onset of fishing or natural mortality in freshwater (Peterman and Dorner 2012). However, we note that there may be errors in aging, stock assignment, and so forth, and these errors may have been greater in the earlier decades of data collection.

For each model run, we could specify three parameters related to environmental variability: (1) the spread of the spawning age distribution (σ_p), (2) the amount of variability in growth (σ_g) and (3) the amount of variability in survival (σ_s). Ideally we would match the values of those factors in the model to the range of values for those factors in the real data sets. However, it is not possible to directly estimate both survival and the spawning age distribution from the available data sets, essentially because we have only a single observation per fish (its age at spawning) and thus more unknowns than data points. For example, an overabundance of age-3 spawners could occur due to high survival or early maturation of that cohort (or both), but it is not possible to distinguish those possibilities with a single datum. Instead we calculated three proxy variables that we used to compare the effects of environmental forcing in the model to variations in the actual data.

From the available spawning-age distribution data, we calculated the mean age of spawning, the standard deviation of the spawning age distribution, and the number of successfully spawning offspring per spawner for each available cohort. These calculations were not possible for the final five years of each time series, because they depended on the abundance of returning adults 3–5 years after they were spawned. Then: (1) the coefficient of variation in the mean age of spawning (CV_{age}) was used to represent the age variability produced by variability in model growth rate (σ_g); (2) the median standard deviation of the spawning (sub-

script sp) age distribution ($\tilde{s}_{sp}$) was used to represent variability due to the spread about the spawning age distribution (σ_p), and (3) the coefficient of variation in recruits per spawner (CV_{rps}) was used to represent the variability in survival within the model (σ_s). We calculated these three statistics in the same way in the model and the data.

In order to compare model-specified values of persistence, P, to the data, we calculated an equivalent statistic for each stock. We used nonlinear least squares to fit a Beverton-Holt spawner–recruit function ($R_{data} = \alpha S/(1 + \beta S)$) to each data set, where S is spawners and R_{data} is subsequent recruits from that cohort of spawners. Here we use the subscript in R_{data} to distinguish observed recruits from the "recruits" (R) used in the simulation model (Eq. 1). In the model, we are able to define recruits as young of the year (age 1), but in the data sets it is only possible to count recruits when they return to freshwater to spawn, so they are age ≥ 3.

To obtain a quantity similar to P to define the proximity of a population to collapse, we note that at equilibrium, the slope of the line running from the origin to the equilibrium point would have slope R/S, and for a population close to collapse this slope would be closer to α, the slope of the spawner–recruit curve at the origin. Thus a population at the extinction threshold would have $R/S = \alpha$, or $\alpha S/R = 1$. We therefore calculated $P_{data} = \log_{10}(\alpha S/R_{data})$ for each stock, yielding a quantity analogous to P for the model simulations. For this calculation we used the average value of S/R_{data} across all years of the data set in order to obtain a single point estimate of P_{data}.

Spectral analysis

We used wavelet spectra (Torrence and Compo 1998) using the Morlet mother wavelet to characterize variability over time in the presence and frequency of population cycles in both real and simulated time series. Wavelet analysis is an extension of spectral analysis (Byrne 2005; for an application to population dynamics, see Grenfell et al. 2001). The goal of a spectral analysis is to identify the dominant frequencies comprising a time series. This is determined by calculating how much of the variance in the time series is associated with different frequencies (this is commonly done using the Fourier transform). For example, a time series with a very consistent period-4 signal (e.g., Late Shuswap; Fig. 1A) would have a frequency spectrum in which most of the variance in found at period 4 (or frequency of 1/4). Wavelet analysis is effectively a localized spectral analysis, in that instead of estimating the frequency spectrum of the entire time series, it estimates the frequency spectrum at each point in the time series. The process is analogous to the calculation of a weighted moving average for a time series. The advantage of wavelet analysis is that it reveals changes in the frequency content of a time series through time, rather than only examining characteristics of the entire time series (Grenfell et al. 2001). For example, the Raft stock (Fig. 1C) was not cyclic between 1950 and 1980, but began to exhibit period-4 cycles in the late 1980s. The wavelet spectrum (Fig. 1J) reveals this: for the noncyclic period, no period stands out as having particularly high variance, but in the late 1980s, there is a peak of variance at period 4. By contrast, the wavelet for Late Shuswap (Fig. 1H) shows consistently high variance at period 4 across the entire time series, as we would expect from inspecting the time series itself (Fig. 1A). Thus wavelet analysis can be used to differentiate time series that are consistently cyclic from those in which cycles start or stop, and can reveal the relative intensity of the cycles (how much variance is represented by a particular frequency).

Statistical significance of peaks in the spectrum was calculated by comparison to a red-noise spectrum with the same autocorrelation as the time series being evaluated. We followed Torrence and Compo's (1998) procedure for calculating the cone of influence, which demarcates the values at the beginning and end of the time series for which the estimate of the wavelet spectrum has a lower sample size because of proximity to the edge. Wavelet calculations were performed on $\log_{10}$-transformed time series so that we could detect the spectra of signals even though mean values changed substantially from year to year within a population and differed greatly among populations.

Quantifying cyclic dominance

In order to quantitatively compare simulation output to empirical data, we developed two metrics for the degree of cyclic dominance and cyclic consistency in a time series of spawner densities. Both were computed from the wavelet analysis of each time series.

We characterized consistency as the proportion of a time series exhibiting cycles at period T ($T = 4$ years for Fraser River stocks and for our simulations; $T = 5$ years for Bristol Bay stocks). We measured this by calculating the wavelet spectrum of the time series ($\log_{10}$-transformed spawner abundances) to obtain variance $W_{k,t}$ at wavelet period k and time t. Variance at period T is then $W_{T,t}$, and the relative variance at T is

$$W'_{T,t} = \frac{W_{T,t}}{\sum_{k=1}^{K} W_{k,t}}$$

where K is the maximum period considered; this scales the metric to make it independent of the overall variance. We then calculated a measure of consistency, C, which is similar to the inverse of the coefficient of variation of $W'_{T,t}$:

$$C = \frac{\bar{W}'_{T,t}}{1 + [\mathrm{var}(W'_{T,t})]^{0.5}}$$

that is, the mean of $W'_{T,t}$ (averaged over the time series) divided by one plus its standard deviation. This statistic tends to 1 for time series dominated by cycles with period T, and to 0 for time series without period T content. The mean and standard deviation are calculated only for the portion of the time series that lies within the cone of influence. For the simulations and for Fraser River sockeye data, $T = 4$ years; for Bristol Bay sockeye data, $T = 5$ years.

We characterized dominance as the degree to which a cyclic time series exhibits a pattern with a single dominant cycle line. Because the cycle phase differs among populations, this is calculated using a moving-window approach. Within a window of four consecutive years, the maximum population density within the window is identified, and the mean difference, d, between the maximum value and all other values in the window is calculated. The window advances through the time series with an increment of 1 year, and dominance, D, is the mean of d over all windows. D has a minimum value of zero but is unbounded from above. This statistic is calculated using $\log_{10}$-transformed data, and is only calculated for the portion of the time series for which the wavelet spectrum exhibits maximum power at period T (that is, the portions of the time series that exhibit period-T cycles). In Fig. 1, the values of C and D as well as the wavelet spectra are shown as an example of these calculations for actual data; the same procedures were applied to simulations.

Results

Presence of cyclic dominance in stochastic simulations

We first examined how the 18 populations of sockeye salmon in the tributaries of the Fraser River and nine populations from Bristol Bay were distributed over our defined characteristics of cyclic dominance, D, and cyclic consistency, C. Plotting both characteristics based on historical data for these stocks (Fig. 2) showed the range of variability of each characteristic. The two characteristics were roughly correlated, as would be expected from their definitions.

We then plotted the values of C and D for each simulated model time series. These simulated values overlapped with values of C and D observed in real sockeye data (Fig. 2). High values of C and D that are consistent with highly cyclic-dominant populations (e.g., Quesnel and Late Shuswap stocks) were predominantly obtained from simulations in which the population was very close to the persistence threshold, P (i.e., $0 < P < 0.08$). In other words, these highly cyclic simulated populations fell on the linear portion of the stock–recruitment relationship, and so had nearly linear dynamics, as would be expected based on earlier results by Myers et al. (1998) and Worden et al. (2010). Many simulations exhibited somewhat less extreme cyclic dominance, with values of C and D similar to stocks that were only cyclic for a portion of the time series, such as Kvichak, Stellako, and Raft. These dynamics were obtained in simulations with a much wider range of persistence values ($0 < P < 0.2$) than the extremely cyclic simulations (Fig. 2). Finally, parameter combinations that were far from the persistence threshold ($P > 0.20$) tended to be acyclic (note the high density of red in the lower left corner of Fig. 2), with low values of C and D, like the Alagnak stock (Fig. 2).

Examination of time series from these model runs (Fig. 3) revealed that the model results were similar to the observed time series (Fig. 1). In Fig. 3 we show representative time series from each quadrant of Fig. 2: consistent cycles with high dominance (high D and C; Fig. 3A), intermittent cycles with high dominance (high D but low C; Fig. 3B), consistent cycles that do not exhibit strong dominance (high C but low D; Fig. 3C), and the absence of period T cycles (low C and D; Fig. 3D). Note that the time series in Fig. 3A bears a strong resemblance to the consistently cyclic-dominant Fraser River stocks (e.g., Late Shuswap; Fig. 1A), and was obtained with relatively low persistence (P), high variance in juvenile survival (σ_m), and low variance in mean age at spawning (σ_g). The other model time series (Fig. 3B–D) are also similar to observed time series in Fig. 1 with similar values of C and D (in Fig. 2 we indicate the location of the simulations shown in Fig. 3): Raft (cf. Figs. 1C and 3B), Kvichak (cf. Figs. 1D and 3C), and Alagnak (cf. Figs. 1E and 3D).

Effects of environmental forcing on cyclic dominance

In order to evaluate the effects of environmentally forced variability in survival and growth on cyclic consistency and dominance, we examined two sets of parameter values: first, those that produced simulations with values of $C > 0.4$ and $1.5 < D < 2.5$, the range of C and D values associated with the two most cyclic-dominant Fraser River stocks (Fig. 2); and second, the parameter combinations that produced simulations with $0.2 < C < 0.4$ and $0.6 < D < 1.5$, a range that encompasses many of the stocks with more moderate patterns of cyclic dominance (Fig. 2).

Extremely cyclic-dominant simulations ($C > 0.4$, $1.5 < D < 2.5$) were only produced by specific values of the parameters we examined (Fig. 4). Specifically, simulations producing extreme cyclic dominance were more likely with: (1) lower persistence ($P < 0.24$), with a median value of $P = 0.05$ (Fig. 4A; recall that P was not specified directly as a model parameter but is determined jointly by all of the deterministic demographic parameters); (2) higher survival forcing (median $\sigma_s = 1.1$; Fig. 4C); and (3) smaller width of the spawning age distribution ($\sigma_p < 0.2$, with median $\sigma_p = 0.05$; Fig. 4G). There was little dependence on growth forcing, with only a slight trend toward lower values (median $\sigma_g = 0.1$; Fig. 4E).

There also was some covariability in the parameter combinations that produced extremely cyclic-dominant dynamics (Fig. 5). Cyclic-dominant simulations with

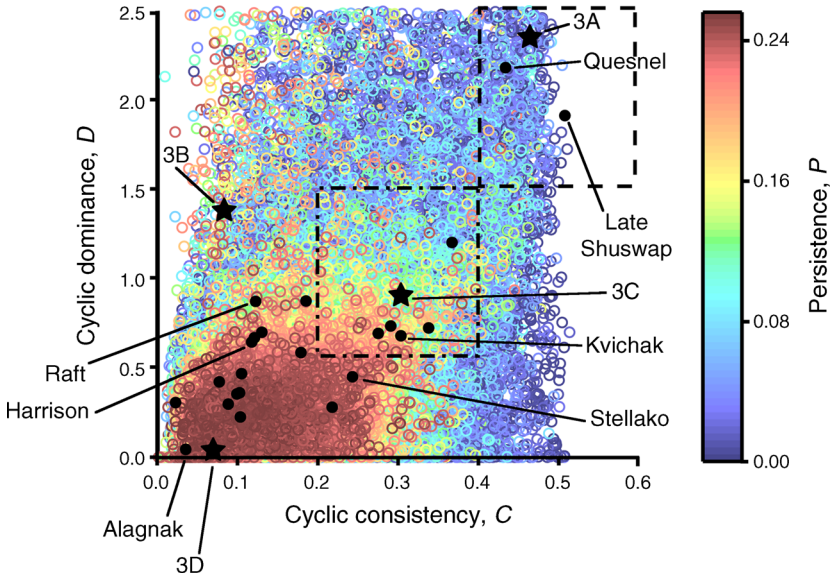

FIG. 2. Cyclic consistency (C) and cyclic dominance (D) of simulated sockeye salmon time series (open symbols) and real sockeye salmon data (black closed symbols). Each point shows the median value of C, D, and population persistence (P, indicated by color) for the set of 100 stochastic simulations with a particular combination of parameter values. Persistence, P, is an estimate of the average proximity of the population to extinction during the time series, based on the average spawning stock size and the shape of the spawner–recruit curve (values closer to 0 are closer to collapse). Data points corresponding to the actual stocks shown in Fig. 1 are labeled. Simulated time series shown in Fig. 3 are marked with stars and labeled according to the respective panel in Fig. 3. Note that some simulations with $D > 2.5$ are not shown, and not all simulations are visible because of overlapping points in the center of the figure. The dashed box demarcates values considered to be extremely cyclic dominant; the dot-dashed box demarcates values considered to be moderately cyclic dominant.

higher values of persistence (P) were primarily associated with: (1) much smaller spawning age spread (σ_p; Fig. 5A) and (2) higher levels of survival forcing (σ_s; Fig. 5C). Also, few simulations produced cycles with both high σ_p and low σ_s (Fig. 5D). There was no other strong covariability among the parameters producing extreme cyclic dominance (Fig. 5B, E, F).

Simulations with only moderate levels of cyclic dominance ($0.2 < C < 0.4$, $0.6 < D < 1.5$) were produced by a much broader range of parameter values than the extremely cyclic-dominant simulations. Moderately cyclic-dominant dynamics were possible with higher levels of persistence (P; Fig. 4B) and spawning age spread (σ_p; Fig. 4H) and lower levels of survival forcing (σ_s; Fig. 4D) than the more extreme cyclic-dominant simulations. The patterns of covariability among parameter combinations producing moderate cyclic dominance (Fig. 6) were nearly identical to the patterns for extreme cyclic dominance (Fig. 5), but the moderate dynamics were obtained over a larger region of parameter space (Fig. 6).

It is important to note that a particular combination of parameter values may make it possible to obtain cyclic-dominant dynamics, but does not guarantee that cyclic dominance will occur. Indeed, one conclusion that can be gleaned from Figs. 4–6 is that cyclic dominance was relatively rare in our simulations (note that the black bars in Fig. 4 are shown five or 10 times higher than their actual value in order to increase their visibility in the figure). For the parameter combinations that most often produced cyclic-dominant dynamics, <7% of simulations were extremely cyclic dominant (e.g., Fig. 5A) and <30% of simulations were moderately cyclic dominant (e.g., Fig. 6A). This is because of the stochastic nature of this mechanism: specific types of environmental perturbations are required to initiate cyclic-dominant behavior. We explore these mechanisms in the next section. We caution that the frequency of cyclic dominance in our simulations should not be compared directly to the frequency of that type of dynamics in real data sets, because the frequency depends heavily on the range of parameter values that we used in our simulations. Nonetheless, one may conclude that having the parameters that favor cyclic dominance does not guarantee that a population will exhibit cycles.

What causes cycles to start and stop?

In order to better understand what types of stochastic variation caused a shift either into or out of extremely cyclic-dominant behavior, we performed additional deterministic simulations that had low values of persistence ($P = 0.01$) and spawning age width ($\sigma_p = 0.15$) and no variation in survival or growth (i.e., $\sigma_g = \sigma_s = 0$), except for single deviations in survival or spawning age in specified years (Figs. 7 and

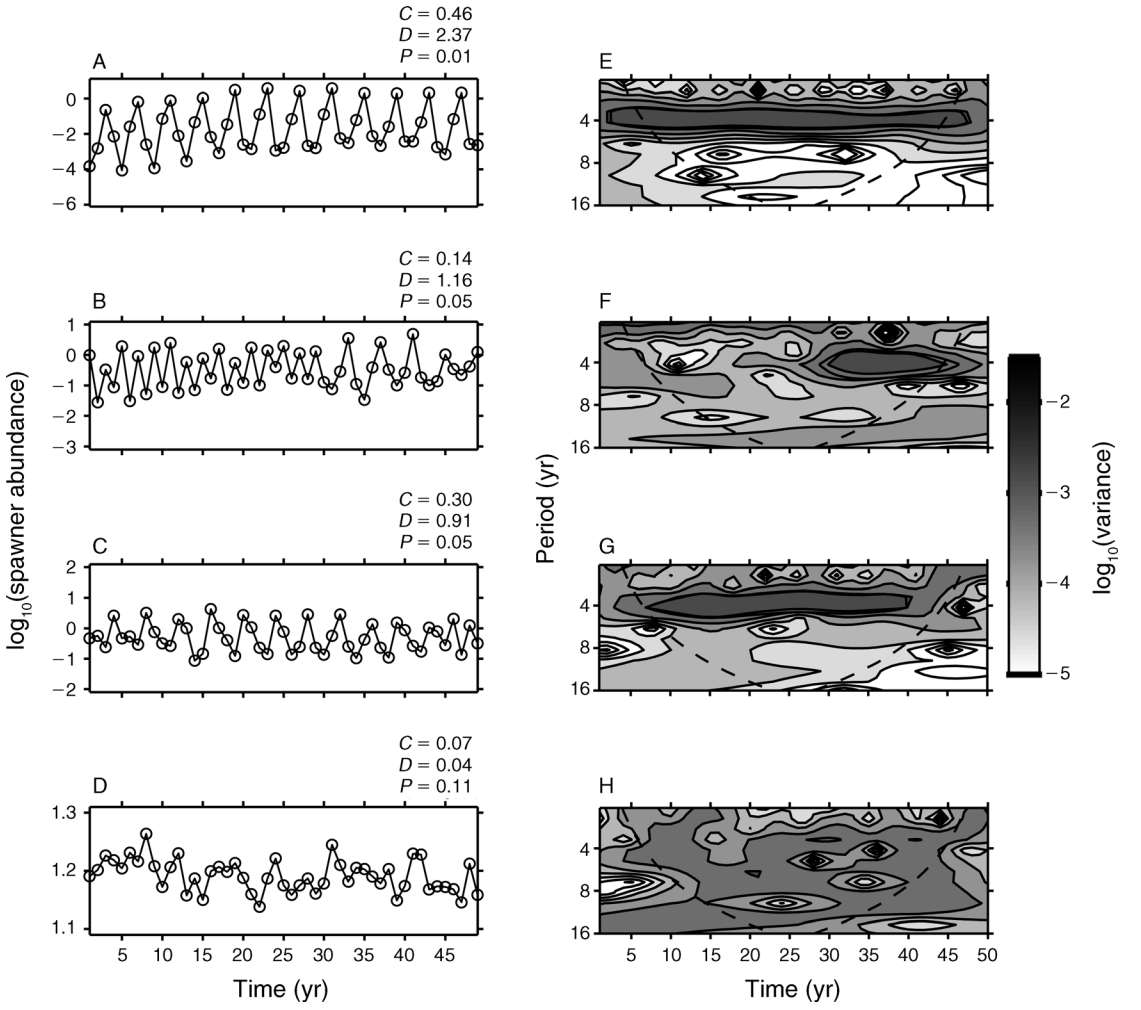

FIG. 3. (A–D) Representative time series and (E–H) corresponding wavelet spectra of simulated sockeye salmon population dynamics. For each simulation, the values of cyclic consistency (C), cylic dominance (D), and persistence (P), are given. The values of C and D indicate the position of each simulation on Fig. 2. The forcing parameters used to create each time series were σ_s (coefficient of variation in juvenile survival), σ_g (coefficient of variation in mean age of spawning), and σ_p (standard deviation of the spawning age distribution), with the following values, by panel: (A, E) $\sigma_s = 0.9$, $\sigma_g = 0.1$,$\sigma_p = 0.15$; (B, F) $\sigma_s = 1.1$, $\sigma_g = 0.05$, $\sigma_p = 0.2$; (C, G) $\sigma_s = 0.4$, $\sigma_g = 0.25$, $\sigma_p = 0.1$; (D, H) $\sigma_s = 0.1$, $\sigma_g = 0.0$, $\sigma_p = 0.45$. Note the differing vertical axis scales in panels A–D. Lines and units in panels E–H are as in Fig. 1.

8). It is not feasible to conduct an exhaustive analysis of all possible conditions that could start or stop cycles in this system, but we provide several examples that illuminate the results of the stochastic simulations that we have presented.

When a deterministic time series with low P experiences a single year of either slightly higher (Fig. 7A) or very high juvenile survival (s_J; Fig. 7B), it produces a spike of the same magnitude in spawner abundance that propagates for many generations with period T (Fig. 7A–D), although only very large positive deviations in survival produce a dominant line that is greater than an order of magnitude more abundant than the subordinate lines (Fig. 7C, D). Negative deviations in survival also produce cycles, but with a single subordinate line instead of a single dominant line (Fig. 7E, F). Small deviations in age at spawning do not noticeably affect the population dynamics (Fig. 7G, H). Larger deviations in age at spawning, both positive (Fig. 7I, J) and negative (Fig. 7K, L), do produce period-4 cycles, but the cycles do not have a single dominant line and three lower-abundance lines as in the Fraser River populations; rather there is a single very-high-abundance and a single very-low-abundance line, with two intermediate-abundance lines between them (Fig. 7G–L).

Adding additional variations in survival or growth to the deterministic simulations can either produce patterns much more like the cyclic-dominant Fraser River stocks, or can stop regular cycles altogether. As examples of the latter, two out-of-phase positive deviations in survival produce a pattern of dominant and subdominant cycle

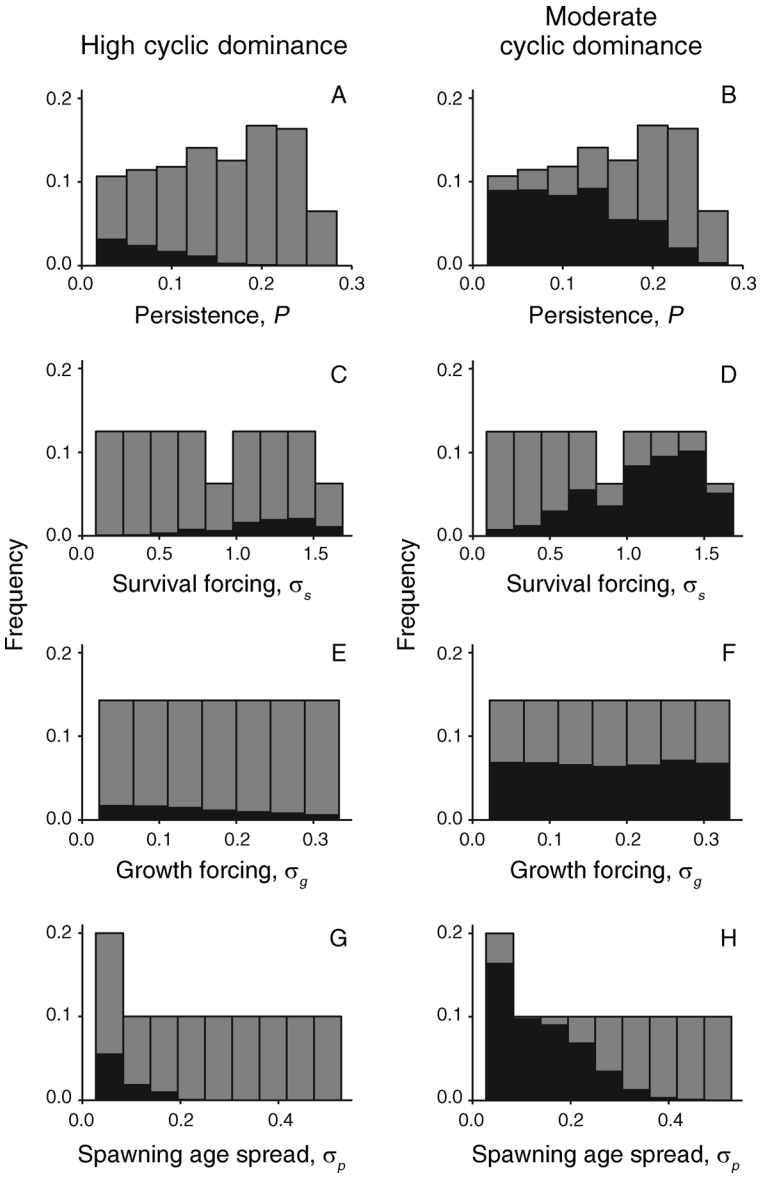

FIG. 4. Distributions of model parameter values producing cyclic-dominant simulations. Gray bars indicate the full distribution of model parameters used in simulations, and black bars indicate the distribution of parameters producing (A, C, E, G) extreme cyclic dominance, defined as $C > 0.4$ and $1.5 < D < 2.5$, or (B, D, F, H) moderate cyclic dominance, defined as $0.2 < C < 0.4$ and $0.6 < D < 1.5$. Each panel corresponds to a model parameter; in panels (A, B) persistence (P) is a composite parameter that depends on the lifetime egg production (LEP) relative to the replacement threshold. Note that the black bars have been increased in height by a factor of 10 in the left-hand panels and a factor of 5 in the right-hand panels to improve visibility.

lines (Fig. 8A, B), like the pattern in Late Shuswap (Fig. 1A, H). Depending on the phase, a negative deviation in survival can either reinforce (Fig. 8C, D) or disrupt (Fig. 8E, F) cycles started by a positive survival deviation. Either positive or negative deviations in growth following a survival deviation can produce cycles very much like those in cyclic-dominant Fraser River stocks (Fig. 8G–J) compared to Late Shuswap (Fig. 1A, H) and Quesnel (Fig. 1B, I). Finally, an overall increase in mean juvenile survival, which raises the value of P, dampens cycles and leads to an increase in abundance (Fig. 8K–L). This is consistent with the result that cyclic dominance was more common in stochastic simulations with low values of P (Fig. 2), and is similar to patterns in Fraser River populations such as Chilko (Appendix: Fig. A1E–F), Gates (Appendix: Fig. A1K, L), and Portage (Appendix: Fig. A1Q, R). Overall, these example simulations suggest that cyclic-dominant dynamics can arise from large positive deviations in survival, possibly accompanied by small (but not large) deviations in growth, and that out-of-phase variation or increases in overall productivity can dampen cycles.

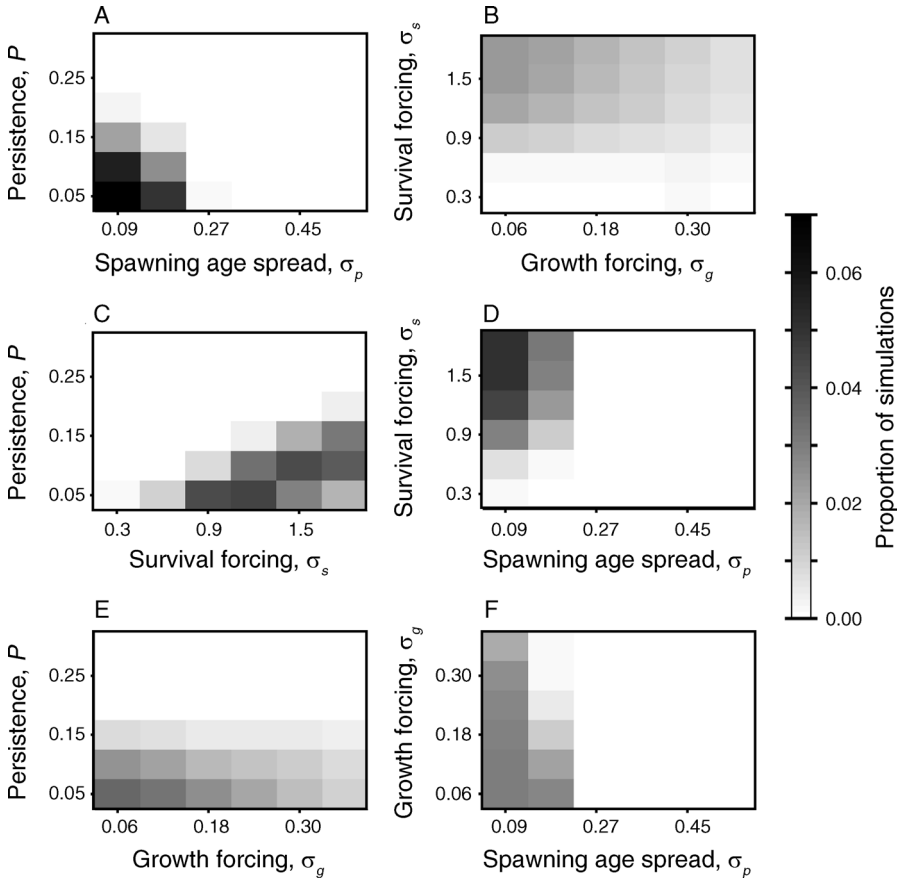

FIG. 5. Combinations of model parameters producing extremely cyclic-dominant simulations. In each panel, shading indicates the proportion of simulations with that range of parameter values that exhibited extreme cyclic dominance, defined as $C > 0.4$ and $1.5 < D < 2.5$.

Levels of forcing in salmon data

The stochastic simulations that we have described so far (Figs. 2–6) can produce patterns of cyclic dominance similar to those in Fraser River populations, given particular ranges of variation in survival and growth. This leads one to ask whether variation in survival and growth in real populations fall within that range. As described in *Methods: Data*, we were not able to directly compare forcing parameters specified in the model to quantities observable in nature. Instead we calculated the proxy variables CV_{rps} (coefficient of variation in recruits per spawner), CV_{age} (coefficient of variation in mean age at spawning), and $\tilde{s}_{sp}$(median standard deviation of the spawning age distribution) for both model and data time series (Table 2).

We examined the values of each of the proxy variables (CV_{rps}, CV_{age}, and $\tilde{s}_{sp}$) for model runs with a range of values of the model-specified parameters σ_s, σ_g, and σ_p, respectively. In each case, we held the other model parameters constant in order to relate the model-specified forcing parameter to the observed proxy variable (Fig. 8). We then examined the relationship between each parameter and the proxy to determine whether the values of the parameter that produced extremely cyclic-dominant simulations (i.e., the values shown in the left-hand panels of Fig. 4) also produced values of the proxy variables that were observed in real cyclic-dominant populations. In other words, were the levels of variability in the model consistent with what could be present in real cyclic-dominant populations?

There was a positive, but nonlinear, relationship between each of the three parameters, σ_s, σ_g, and σ_p, and its corresponding, empirically estimated proxy variable (Fig. 9). Moreover, in each case, many of the simulations generated with parameter values in the range that produced extremely cyclic-dominant simulations (i.e., $C > 0.4$, $1.5 < D < 2.5$) also had values of the proxy variables that fell within the range observed in Fraser River and Bristol Bay stocks. These values overlapped the median value for the Quesnel and Late Shuswap stocks, the two most cyclic-dominant stocks (Fig. 9).

We note that many stocks that do not exhibit extreme cyclic dominance have values of the three proxy variables that are similar to those of Quesnel and Shuswap, and thus may be experiencing similar levels of

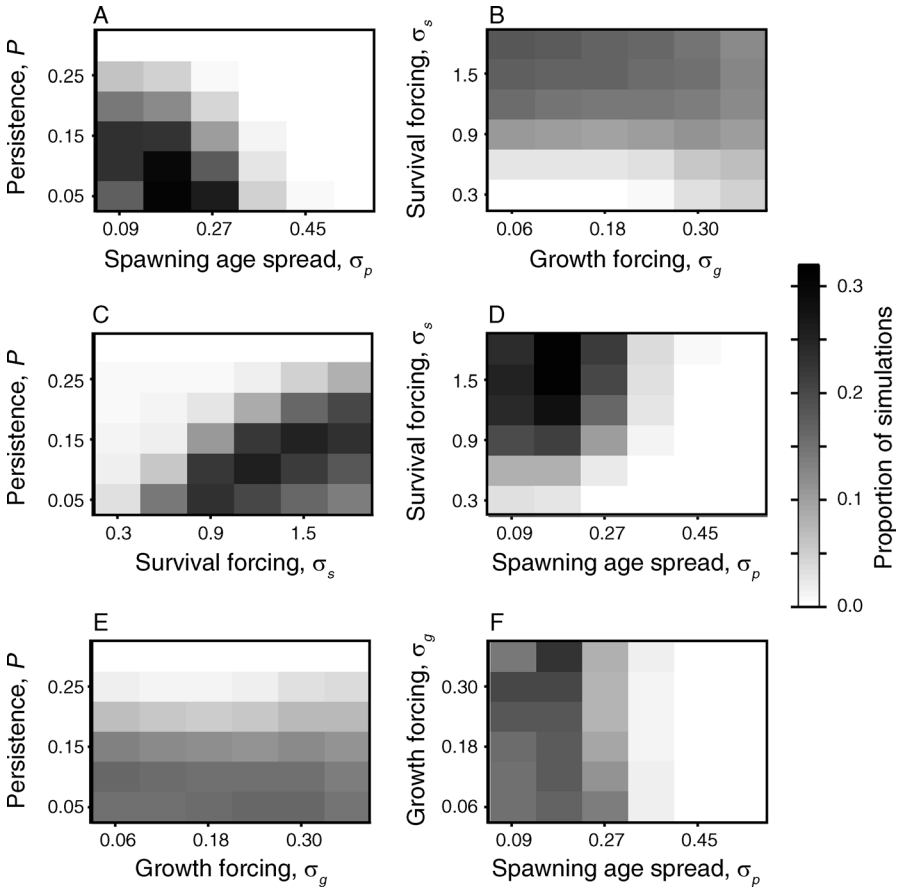

FIG. 6. Combinations of model parameters producing moderately cyclic-dominant simulations. In each panel, shading indicates the proportion of simulations with that range of parameter values that exhibited moderate cyclic dominance, defined as $0.2 < C < 0.4$ and $0.6 < D < 1.5$.

environmental forcing without producing cycles. This is consistent with the results of the simulations. For example, although cyclic dominance was only produced by high levels of survival forcing, not every simulation with high survival forcing exhibited cyclic dominance during the portion of the time series that we examined (Fig. 4B). Thus, one reason a real stock may not exhibit cyclic dominance, despite high levels of environmental variability, is that it simply may not have experienced a forcing event sufficient to produce cycles (such as the examples in Figs. 7 and 8). Other reasons are that the stock may have sufficiently high LEP that density-dependent interactions rapidly dampen any cycles, or the spawning age distribution may be relatively broad, limiting cohort resonance.

The simulations predict that extreme cyclic dominance occurs predominantly when stocks are near the persistence threshold and exhibit linear dynamics. To test that, we calculated values of persistence, P_{data}, from the historical data for stock, and compared them to each stock's relative cyclic dominance (i.e., their values of C and D). Consistent with the simulation results, only stocks with low persistence ($P_{\text{data}} < 0.4$) exhibited high values of C ($C > 0.2$) and D ($D > 0.8$) (Fig. 10). For example, the cyclic-dominant Late Shuswap stock has a gently sloping spawner–recruit relationship, and the average spawner density falls on a nearly linear portion of the curve (Fig. 10A). This stock is near the persistence threshold and does have extremely cyclic-dominant dynamics. By contrast, the Harrison stock has a much steeper spawner–recruit curve (Fig. 10B), such that the average spawner density falls on the flat, asymptotic portion of the curve. Thus variability in growth and survival will be dampened by density-dependent processes, and this stock would not be expected to have cycles, as observed. An important feature of these distributions is that some stocks with low values of P_{data} did not exhibit cycles (Fig. 10), indicating that a low value of P_{data} creates the possibility of cycles, but in the absence of the necessary forcing or a sufficiently narrow spawning age distribution, they may not have started cycling. Note that we refrain from directly comparing values of P_{data} calculated from data and values of P calculated for models because the two quantities are calculated in a different manner, despite having the same general meaning.

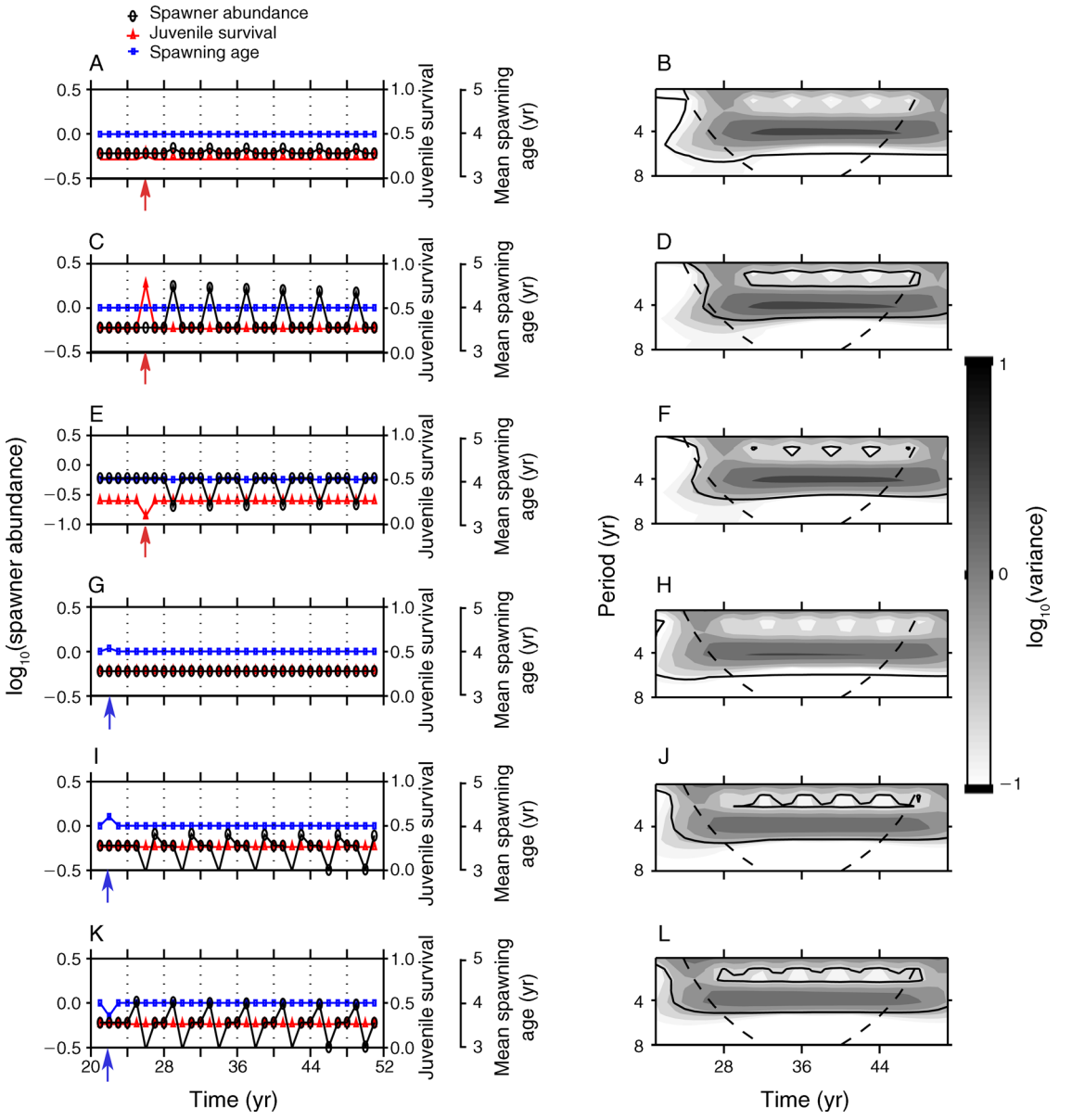

FIG. 7. Non-stochastic model simulations with single forcing events. Each left-hand panel displays a portion of a 60-year model time series, showing $\log_{10}$-transformed spawner abundance (left axis, black lines and ovals), juvenile survival (right axis, red line and triangles), and the mean age at spawning for each cohort (second right axis, blue line and squares). Because forcing events affect juveniles, there is a time lag before effects appear in the spawner time series. The corresponding wavelet spectrum is shown on the right; symbols are as in Fig. 1. For clarity, the arrow below each axis also indicates when the forcing event occurs, and the arrows are color-coded according to the type of forcing. Note that in the left-hand panels, the left axes change scale among panels, but both right axes keep the same scale.

DISCUSSION

We obtained a set of four results that, taken together, indicate that cohort resonance produces cyclic-dominant behavior in sockeye salmon and reveal the conditions under which that behavior occurs. First, stochastic simulations of age-structured models indicated that cyclic dominance occurred only within a particular range of values for three parameters: (1) lifetime egg production, (2) spawning age distribution, and (3) stochastic variability in juvenile survival. Within that range of values, lower values of (1) and (2) and higher values of (3) produced more extreme cyclic dominance. Second, simulations with different types of environmentally forced variability revealed that isolated, large, positive deviations in survival were needed to initiate cyclic dominance, but that less dramatic perturbations could disrupt cycles. Third, model simulations over the range of the three parameters that produced extreme

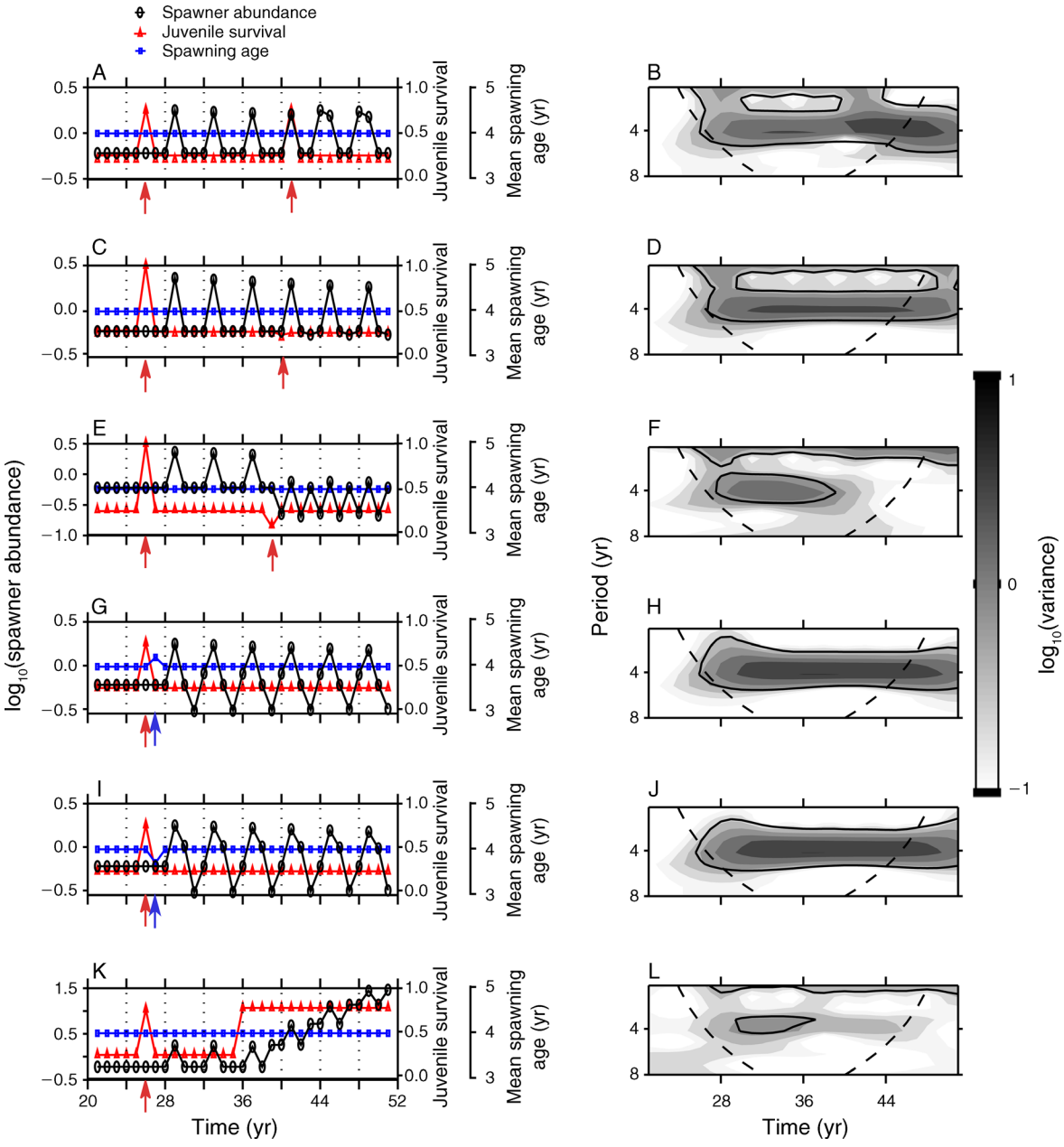

FIG. 8. Non-stochastic model simulations with multiple forcing events. Each left-hand panel displays a portion of a 60-year model time series, showing spawner density (left axis, black lines and ovals), juvenile survival (right axis, red line and triangles), and the mean age at spawning for each cohort (second right axis, blue line and squares). Because forcing events affect juveniles, there is a time lag before effects appear in the spawner time series. The corresponding wavelet spectrum is shown on the right; symbols are as in Fig. 1. For clarity, arrows below each axis also indicate when the forcing event occurs, and the arrows are color-coded according to the type of forcing. Note that, in the left-hand panels, the left axes change scale among panels, but both right axes keep the same scale.

cyclic dominance yielded values of proxy variables that fell within the range of values observed in real data. Finally, the actual populations exhibited the same relationship with persistence identified by the model: high values of both cyclicity and dominance occurred only in populations with low values of persistence (i.e., low LEP). This occurs because, at very low LEP, the population occupies the linear, ascending portion of the spawner–recruit relationship, producing nearly linear, density-independent dynamics that are more sensitive to stochastic environmental forcing. This implies that, all else being equal, populations exhibiting this type of cycle are closer to extinction than noncyclic populations, and that cyclic behavior could precede population collapse.

TABLE 2. Time series statistics for Fraser River and Bristol Bay populations of sockeye salmon.

Stock, by region	P_{data}	C	D	CV_{rps}	CV_{age}	$\tilde{s}_{sp}$
Fraser River						
Birkenhead	1.16	0.08	0.42	0.95	0.05	0.49
Bowron	1.03	0.18	0.88	0.80	0.04	0.24
Chilko	1.40	0.18	0.59	1.05	0.02	0.30
Cultus†		0.29	0.74			
Early Stuart	0.82	0.13	0.70	0.87	0.02	0.21
Fennell	1.19	0.13	0.57	1.29	0.04	0.24
Gates	0.84	0.22	0.64	1.14	0.05	0.24
Harrison	0.58	0.12	0.67	1.48	0.06	0.42
Late Shuswap	0.73	0.51	1.91	1.03	0.05	0.17
Late Stuart	0.49	0.28	1.57	1.68	0.03	0.19
Nadina	0.82	0.19	1.00	0.85	0.03	0.01
Pitt	1.26	0.02	0.31	0.89	0.04	0.44
Portage	0.80	0.26	0.60	1.52	0.02	0.17
Quesnel	0.75	0.43	2.18	0.93	0.04	0.12
Raft	0.87	0.12	0.87	0.87	0.05	0.36
Scotch†				0.75	0.02	0.02
Seymour	0.81	0.34	0.73	1.01	0.03	0.14
Stellako	1.17	0.24	0.45	0.69	0.03	0.31
Weaver	1.00	0.02	0.22	0.98	0.03	0.27
Bristol Bay						
Alagnak	1.79	0.03	0.04	1.25	0.06	0.54
Egegik	0.69	0.10	0.23	0.69	0.03	0.56
Igushik	6.53	0.10	0.47	1.12	0.03	0.48
Kvichak	1.12	0.30	0.68	0.89	0.05	0.53
Naknek	1.51	0.22	0.28	0.53	0.04	0.60
Nushagak‡	19.67			0.62	0.05	0.57
Togiak	2.65	0.09	0.30	0.57	0.03	0.54
Ugashik	1.41	0.12	0.65	1.11	0.05	0.57
Wood	1.91	0.10	0.36	0.49	0.04	0.54

Notes: P_{data} is an estimate of average proximity of the population to extinction during the time series, based on average spawning stock size and shape of the spawner–recruit curve (values closer to 0 are closer to collapse). C and D were calculated from the wavelet spectra of the time series. C is a measure of how consistently the spectrum had high power at the dominant period (four years for Fraser River, five years for Bristol Bay). D is a measure of how dominant one cycle-line was over the other cycle lines during periods of cycling at the dominant period. CV_{rps} is the coefficient of variation of recruits-per-spawner, a measure of interannual variability in juvenile survival; CV_{age} is the coefficient of variation of mean age at spawning for each cohort, a measure of interannual variability in growth; $\tilde{s}_{sp}$ is the median standard deviation of the spawning age distribution, a measure of average spread in the spawning age.

† No spawning age data were available, so it was not possible to calculate some statistics.

‡ The time series was too short to calculate C and D.

The set of conditions that make extreme cyclic dominance possible in our simulations also suggest why these dynamics are only observed in a few sockeye salmon populations. Strong cohort resonance requires a narrow spawning age distribution, so this type of cycle should emerge primarily in semelparous species with a very consistent life span. Sockeye salmon in the Fraser River meet this requirement, because they nearly always spawn at age 4 years. Bristol Bay sockeye have a broader age distribution, with some species delaying spawning until age 6 years, and cyclic dominance is less common in those stocks. Other salmon species, such as chinook (*Oncorhyncus tshawytscha*) and chum (*O. kisutch*), have a broader distribution of ages at spawning, and are less likely to exhibit strong cycles of this type (Groot and Margolis 1991). Pink salmon (*O. gorbuscha*), on the other hand, have a two-year life span with no overlap between spawning lines. Given that spawning age distribution, the extreme period-2 cycles observed in these stocks (Groot and Margolis 1991) could be driven (or enhanced) by the type of stochastic effects that we have described here (Krkosek et al. 2011). Iteroparous species should be less likely to exhibit strong cyclic dominance, although heavy size-selective fishing could truncate the age distribution of a population enough that the spawning age distribution narrows and cycles become more likely (Botsford et al. 2011).

Relationship between population persistence and cyclic dominance

The finding that cycles are associated with dynamics near the persistence threshold is consistent with prior modeling of salmon population dynamics (Myers et al. 1998, Worden et al. 2010) and with more recent work on early-warning indicators for population collapse in general systems, which states that populations are more variable prior to collapse (Drake and Griffen 2010). Myers et al. (1998) used a deterministic age-structured model to examine cyclic dominance in sockeye salmon, and found that the key parameter affecting the presence of period-T cycles was the slope at the origin of the spawner–recruit curve. This is related to our result, in

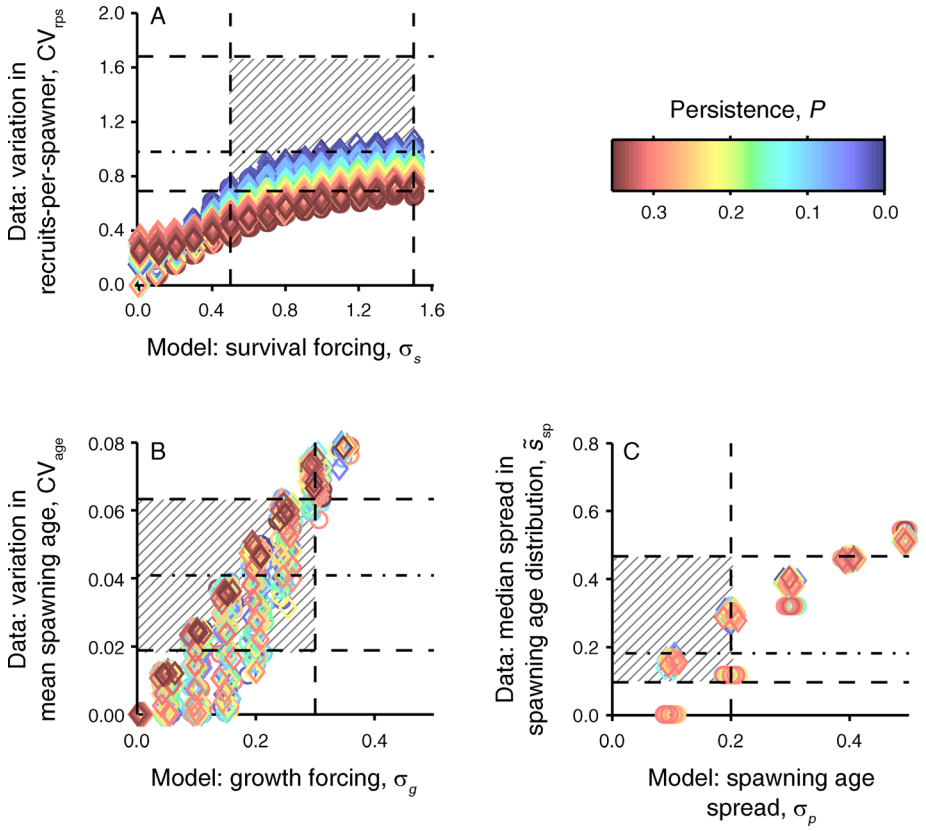

FIG. 9. Comparison between model-specified parameters (σ_s, σ_g, σ_p) and the corresponding proxy variables that can be estimated from data (CV_{rps}, CV_{age}, $\tilde{s}_{sp}$). Vertical dashed lines indicate the range of parameter values that produce cyclic-dominant simulations ($C > 0.4$, $1.5 < D < 2.5$), horizontal dashed lines indicate the range of proxy variables observed in Fraser River and Bristol Bay stocks, and the cross-hatched region indicates the intersection of those two ranges. The horizontal dot-dashed line indicates the mean of each proxy variable for the two most cyclic-dominant stocks (Late Shuswap and Quesnel). Each point represents one simulation and is colored to indicate persistence, P. Simulations were run with $s_A = 0.7$, s_J ranging from 0.1 to 0.5, and in panel (A) variable σ_s, $\sigma_g = 0$ (circles) or 0.5 (diamonds), σ_p ranging from 0 to 0.6; in panel (B) variable σ_g, $\sigma_s = 0$ (circles) or 1.0 (diamonds), σ_p ranging from 0 to 0.6; and in panel (C) variable σ_p, $\sigma_s = 1.0$, $\sigma_g = 10^{-10}$ (circles) or 0.5 (diamonds).

that population persistence requires that LEP be greater than the inverse of the slope (Sissenwine and Shepherd 1987, Botsford 1997), so cycles arise when LEP is very low (our result) or when the slope is very shallow (Myers et al. 1998). More recently, Guill and colleagues (Guill et al. 2011, Schmitt et al. 2012) found that a multispecies model of sockeye dynamics (including the zooplankton prey and trout predators of sockeye fry in rearing lakes) could generate cyclic-dominant cycles, but, as in our model, only in the absence of strong density dependence in the sockeye population. However, our approach improves on these earlier efforts in that we have quantified the cyclic-dominant properties of our simulations rather than merely relying on qualitative visual inspection. As a result, we can more confidently note the similarities between our model dynamics and those of real salmon time series. Prior authors who have relied on visual inspection of the time series (e.g., Myers et al. 1998, Guill et al. 2011, Schmitt et al. 2012) have produced simulations that are qualitatively similar to Fraser River sockeye data, but that lack key features of those time series (dominance of a single cycle line [Myers et al. 1998] and occasional starting and stopping of cycles [Guill et al. 2011, Schmitt et al. 2012]). By contrast, simulations with appropriate values of C and D exhibited all of the characteristic features of both extremely cyclic-dominant Fraser River populations and populations with less extreme cyclic-dominant dynamics (Fig. 3).

If cyclic-dominant behavior occurs primarily when populations are close to the persistence threshold, what does this imply about populations that have been consistently cyclic for many decades without collapsing? A form of selection bias akin to the anthropic principle (Bostrom 2002) or the Prosecutor's Fallacy (Boettiger and Hastings 2012) may be at work here: modern observers do not possess long time series of stocks with similar dynamics that collapsed long ago, so we are only able to observe those stocks that have, by chance, not collapsed. Apparently, cycles in Fraser River sockeye populations were present prior to the arrival of Europeans in British Columbia (Ricker 1950). Conse-

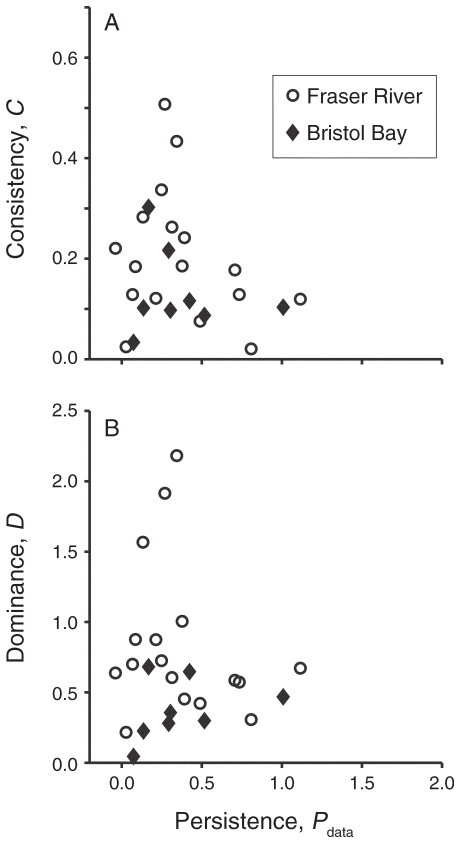

FIG. 10. Relationship between persistence (P_{data}) and metrics of cyclic dominance (A) C and (B) D for Fraser River (open circles) and Bristol Bay stocks (solid diamonds). P_{data} was estimated from empirical spawner–recruit relationships and the mean value of LEP for that stock, and C and D were estimated from time series of spawner abundance.

quently, those cyclic populations were either already reduced to low LEP by harvest by indigenous fishermen (which seems unlikely), or they simply have a highly linear stock–recruit relationship (over the range of observed data), and are limited by some other factor. In any case, some Fraser River populations that were cyclic for long periods have recently reached extremely low abundances (e.g., Late Stuart and Quesnel; Peterman et al. 2010), so it is possible that such populations do stand near the threshold of persistence, and small changes in mean survival (or other factors) can push them toward collapse (in this case, there appears to be a region-wide decline in sockeye salmon productivity over the past decade due to as-yet-unknown factors; Peterman and Dorner 2012). Somewhat cyclic dynamics have also accompanied population collapse in other Pacific salmon populations, e.g., California Central Valley Winter run chinook (Botsford and Brittnacher 1998) and Snake River chinook (Emlen 1995). An example of the inverse of this pattern is Chilko Lake, a previously cyclic Fraser River sockeye population that became noncyclic following lake fertilization, which increased lake productivity and presumably increased juvenile survival and growth (Ricker 1997), but also may have increased density. However, while many Fraser River sockeye stocks have been declining since the 1990s, one of the populations exhibiting the most striking cyclic dominance in the data set that we analyzed, Late Shuswap, has not shown declines in sockeye salmon (Peterman et al. 2010, Peterman and Dorner 2012). Indeed, the recent historically high Fraser River sockeye run in 2010 was primarily the result of the Late Shuswap stock (2010 coincided with the dominant year line; DFO 2010). This does not necessarily conflict with the conclusions from our simulation models, because a variety of local and regional processes may be contributing to the decline of Fraser sockeye stocks, and it is possible that these factors may differ among populations (although it is unlikely that each stock is affected by

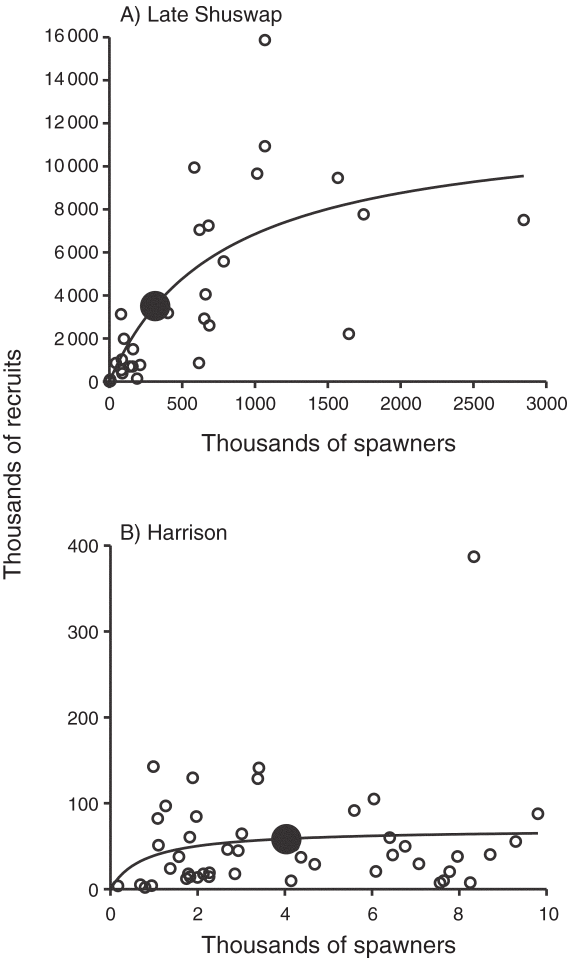

FIG. 11. Spawner–recruit relationships for (A) a cyclic-dominant Fraser stock, Late Shuswap (note that several points appear to overlap near the origin), and (B) a Fraser stock that does not exhibit cyclic dominance, Harrison. Open circles indicate yearly data points; large solid circles indicate the recruitment predicted for mean spawner abundance.

completely independent processes; Peterman et al. 2010, Peterman and Dorner 2012).

When considering the relationship between cyclic dynamics and persistence, it is important to note that the high densities achieved by the dominant cycle line may tend to maintain an extant population, despite the overall proximity to the deterministic persistence threshold. In our calculations of P_{data}, we calculated the mean ratio of recruits per spawner across the time series for each stock. For highly cyclic stocks, this value is associated with high variance, because the dominant cycle line years may move far out onto the asymptotic portion of the spawner–recruit curve even if the mean ratio is close to the persistence threshold (e.g., Late Shuswap; Fig. 11A).

The idea that the likelihood of occasional random forays into cyclic population behavior depends on a population's proximity to the persistence threshold provides a new perspective on research evaluating the portfolio biodiversity effect associated with fluctuating Bristol Bay sockeye populations (Hilborn et al. 2003, Moore et al. 2010, Schindler et al. 2010). The thrust of these analyses is that because these populations vary asynchronously, the variance of the whole assemblage is dampened, providing a more stable fishery resource. These analyses of the portfolio effect are phenomenological in the sense that the description of the portfolio effect depends on means and variances calculated from population abundance, without knowledge of the underlying mechanism causing the effect (Moore et al. 2010, Schindler et al. 2010; but see Greene et al. 2010). Classically, portfolio effects have been attributed to species' (or populations') independent responses to environmental variability (e.g., Tilman et al. 2006). However, our results indicate that the calculated variability in sockeye populations is due, in part, to an endogenous mechanism of population dynamics; furthermore, that mechanism is linked to the probabilities of persistence of individual populations. It seems that analyses including the mechanisms described here would improve our understanding of the sources of relative variability in these sockeye populations, as well as whether all of the stocks in the portfolio can be expected to persist over long time scales.

Sources of environmental stochasticity

Variability in sockeye survival and growth rates could arise either during freshwater residency, after outmigration to the ocean, or both. Our model introduced survival variability in the first year, but because the only nonlinearity in the model is the spawner–recruit relationship, identical results could have been obtained with similar levels of variability in ocean survival. Cyclic Fraser River populations are out of phase with each other, suggesting that the stochastic event that initiated the cycles occurred in the freshwater phase or the early ocean phase, rather than later during the ocean phase when fish from multiple stocks may commingle and experience similar conditions. Stocks also vary in the timing of outmigration (Ricker 1950), so stochasticity during that stage could also introduce phase differences.

Overall survival in sockeye salmon covaries at the regional scale (i.e., within Fraser River stocks) and not at the basin scale, suggesting that there are region-scale marine influences on variability in survival (Peterman et al. 1998). However, within the Fraser River watershed, environmental conditions covary with survival most strongly at time lags that coincide with the initial freshwater residency, suggesting that freshwater processes may introduce the greatest variability in survival (Mueter et al. 2005). By contrast, Pyper et al. (1999) found that length-at-age and age-at-maturity covaried among Fraser River stocks across years, suggesting that marine processes (perhaps during the final ocean year) were primarily responsible for interannual variation in these traits. Thus, variability in survival is more likely to vary among stocks, while variability in growth may be synchronous among stocks, potentially synchronizing their dynamics. These patterns are consistent with our simulation results; we found that stochastic variation in survival, not growth, was more likely to produce cyclic dominance, and that the presence of cyclic dominance was relatively insensitive to the level of year-to-year variability in growth. Thus, spatial covariability in growth rates would be less likely to synchronize cyclic populations. One would also expect life history constraints to preclude large variations in age at spawning (e.g., spawning before age 3 or after age 6), so there should be greater scope for variability in survival than in growth, which is again consistent with the conditions favoring cyclic dominance.

In these simulations, we assumed that environmental stochasticity had a white spectrum (equal variance at all frequencies), but natural variability is typically red-shifted (Halley 1996, Vasseur and Yodzis 2004) and conditions in the North Pacific Ocean may have even more complex spectral content (e.g., Pacific Decadal Oscillation, North Pacific Gyre Oscillation, and El Niño cycles; Di Lorenzo et al. 2010). Our simulations essentially reveal the spectral sensitivity of the population; colored environmental noise would be filtered by the population dynamics, so variability with a period near T should excite the period-T mode of variability seen in our simulations (Greenman and Benton 2005; for examples, see Botsford et al. 2011). Using white-noise forcing spectra in ecological models has been criticized (Heino et al. 2000, Greenman and Benton 2005), but this was a conservative approach to determine whether stochasticity could produce cyclic dominance, given our uncertainty as to the source or timing of important environmental forcing events. Examining the effects of colored environmental noise on sockeye salmon populations could be a productive future line of research; the frequency spectrum of environmental variability affecting the North Pacific may be changing (e.g., Cobb et al.

2003), and sockeye dynamics are sensitive to climatic regime shifts (Beamish et al. 1997).

Many of the Fraser River sockeye time series do exhibit some low-frequency variability at decadal scales or greater (note the high, but statistically nonsignificant, variance at periods >10 yr in Fig. 1). This could reflect the influence of red-shifted environmental stochasticity, or the low-frequency component of the cohort resonance effect (Bjørnstad et al. 1999, 2004, Worden et al. 2010). This component is only evident in very long time series (e.g., ~100 years; Bjørnstad et al. 2004), and so does not appear in our relatively short simulations (Fig. 3). However, it could partially explain the slow, decade-scale decline in Fraser River sockeye population densities.

Implications

Our results suggest the need to account for environmental stochasticity as a source of very regular cyclic dynamics, at least in sockeye salmon, and possibly in other species as well. Population dynamics with strong period-T cycles are typically attributed to deterministic intra- or interspecific interactions, particularly intercohort cannibalism (e.g., flour beetles *Tribolium confusum* [Costatino et al. 1997]; cod *Gadus morhua* [Bjørnstad et al. 1999]; and Eurasian perch *Perca fluviatilis* [Claessen et al. 2000]), and apparent competition among cohorts (proposed for sockeye salmon by Ward and Larkin [1964]; modeled by Guill et al. [2011]). Our simulations show that, given relatively linear dynamics and narrow age structure (including semelparity), similar period-T cycles can emerge as a result of stochastic variability.

Cyclic dynamics due to intercohort interactions are typically represented in population models using delayed density-dependent feedbacks (Nisbet 1997). In the case of sockeye salmon, evaluations of fishery management strategies often include delayed density dependence to approximate cyclic-dominant behavior (e.g., Martell et al. 2008). However, Myers et al. (1997) and Peterman and Dorner (2011) found no evidence for delayed density dependence in Fraser River sockeye populations (with the possible exception of Quesnel), at least at the time lag required to produce period-T cycles. Moreover, some cyclic-dominant populations have the incorrect sequence of dominant and subdominant year lines, such that delayed density dependence does not explain their dynamics (Myers et al. 1997).

One important aspect of the mechanism that we have proposed to explain cyclic-dominant dynamics is its stochastic nature. The various dynamic mechanisms described in the previous two paragraphs are essentially deterministic: if those mechanisms are in place, the population will nearly always exhibit cycles. For example, the three-species system described by Guill et al. (2011) has an unstable equilibrium that bifurcates into a period-4 cycle; a population with those dynamics would cycle indefinitely. By contrast, in our simulations, populations did not necessarily exhibit cyclic dominance, even if the necessary conditions were in place (low persistence, narrow spawning age distribution), unless a suitably timed disturbance occurred to set the cycles into motion. Thus, extreme cyclic dominance was relatively rare in our simulations (Fig. 5), although moderate cyclic dominance with intermittent cycles was somewhat more common (Fig. 6). We argue that this is quite consistent with the observed distribution of cyclic dynamics in real populations: many stocks appear to have the appropriate enabling conditions (low persistence, narrow spawning age distribution, variable survival), but only a few of those exhibit strong cyclic dominance (Fig. 10).

Our finding that cyclic-dominant behavior could originate purely from environmental stochasticity leads to important conclusions for future prediction and management of sockeye populations. Rather than being due to the abundance of older age classes or other species (i.e., things human managers can control), cyclic dynamics may start or stop due to extrinsic factors. From a management perspective, the resulting unpredictability of the year class strength of recruits leads to consistent errors in setting sockeye harvest goals (Holt and Peterman 2007), so a reduction in the intensity of the cycles could be desirable. Martell et al. (2008) suggest possible adaptive management experiments to test for the importance of delayed density dependence and depensatory fishing in producing cycles by using a fallow rotation strategy (deliberately overfishing some cycle lines in an attempt to reestablish a dominant line), or by easing harvest on nondominant cycle lines to reduce depensatory effects. A complementary experiment suggested by our results would be to reduce fishing on all cycle lines to increase lifetime egg production, thus reducing the propensity to cycle. Walters and Staley (1987) originally suggested this management experiment and outlined some of the risks that it entails. Of course, even if this were done, it would be difficult to separate the effects of fishing on population dynamics from other confounding factors. There has been a shift toward lower harvest rates on Fraser River sockeye since the mid-1990s, but this has coincided with a large-scale decrease in spawner productivity and marine survival rates (Peterman and Dorner 2011). This decline precludes a simple test of the relationship between productivity and cyclic dominance at this time.

Acknowledgments

We are grateful to M. Lapointe (Pacific Salmon Commission) for providing Fraser River sockeye data and R. Peterman (Simon Fraser University) for providing Bristol Bay sockeye data, and to both scientists for extremely helpful comments on the manuscript. We thank two anonymous reviewers for helpful suggestions. This research is part of U.S. GLOBEC (U.S. Global Ocean Ecosystems Dynamics) synthesis activities and was supported by National Science Foundation grant NSF OCE0815293.

Literature Cited

Barrowman, N. J., R. A. Myers, R. Hilborn, D. G. Kehler, and C. A. Field. 2003. The variability among populations of coho

salmon in the maximum reproductive rate and depensation. Ecological Applications 13:784–793.

Beamish, R. J., C. M. Neville, and A. J. Cass. 1997. Production of Fraser River sockeye salmon (*Oncorhyncus nerka*) in relation to decadal-scale changes in climate and the ocean. Canadian Journal of Fisheries and Aquatic Sciences 54:543–554.

Bjørnstad, O. N., J.-M. Fromentin, N. C. Stenseth, and J. Gjøsæter. 1999. Cycles and trends in cod populations. Proceedings of the National Academy of Sciences USA 96:5066–5071.

Bjørnstad, O. N., R. M. Nisbet, and J.-M. Fromentin. 2004. Trends and cohort resonant effects in age-structured populations. Journal of Animal Ecology 73:1157–1167.

Boettiger, C., and A. Hastings. 2012. Early warning signals and the prosecutor's fallacy. Proceedings of the Royal Society B 279:4734–4739.

Bostrom, N. 2002. Anthropic bias: observation selection effects in science and philosophy. Routledge, New York, New York, USA.

Botsford, L. W. 1997. Dynamics of populations with density-dependent recruitment and age structure. Pages 371–408 *in* S. Tuljapurkar and H. Caswell, editors. Structured population models in marine, terrestrial, and freshwater systems. Chapman and Hall, New York, New York, USA.

Botsford, L. W., and J. G. Brittnacher. 1998. Viability of Sacramento winter-run Chinook salmon. Conservation Biology 12:65–79.

Botsford, L. W., M. D. Holland, J. F. Samhouri, J. W. White, and A. Hastings. 2011. Importance of age structure in models of the response of upper trophic levels to fishing and climate change. ICES Journal of Marine Science 68:1270–1283.

Botsford, L. W., and D. E. Wickham. 1978. Behavior of age-specific, density-dependent models and the Northern California Dungeness crab (*Cancer magister*) fishery. Journal of the Fisheries Research Board of Canada 35:833–843.

Byrne, C. L. 2005. Signal processing: a mathematical approach. A. K. Peters, Wellesley, Massachusetts, USA.

Caswell, H. 2001. Matrix population models: construction, analysis, and interpretation. Second edition. Sinauer, Sunderland, Massachusetts, USA.

Claessen, D., A. M. de Roos, and L. Persson. 2000. Dwarfs and giants: cannibalism and competition in size-structured populations. American Naturalist 155:219–237.

Cobb, K. M., C. D. Charles, H. Cheng, and R. L. Edwards. 2003. El Niño/Southern Oscillation and tropical Pacific climate during the last millennium. Nature 424:271–276.

Costatino, R. F., R. A. Desharnais, J. M. Cushing, and B. Dennis. 1997. Chaotic dynamics in an insect population. Science 275:389–391.

DFO (Department of Fisheries and Oceans). 2010. Pre-season run size forecasts for Fraser River Sockeye salmon in 2010. DFO Canadian Science Advisory Secretariat Science Advisory Report 2010/031.

Di Lorenzo, E., K. M. Cobb, J. C. Furtado, N. Schneider, B. T. Anderson, A. Bracco, M. A. Alexander, and D. J. Vimont. 2010. Central Pacific El Niño and decadal climate change in the North Pacific Ocean. Nature Geoscience 3:762–765.

Drake, J. M., and B. D. Griffen. 2010. Early warning signals of extinction in deteriorating environments. Nature 467:456–459.

Emlen, J. M. 1995. Population viability of the Snake River chinook salmon (*Oncorhyncus tshawytscha*). Canadian Journal of Fisheries and Aquatic Sciences 52:1442–1448.

Greene, C. M., J. E. Hall, K. R. Guilbault, and T. P. Quinn. 2010. Improved viability of populations with diverse life-history portfolios. Biology Letters 6:382–386.

Greenman, J. V., and T. G. Benton. 2005. The frequency spectrum of structured discrete time population models: its properties and their ecological implications. Oikos 110:369–389.

Grenfell, B. T., O. N. Bjørnstad, and J. Kappey. 2001. Travelling waves and spatial hierarchies in measles epidemics. Nature 414:716–723.

Groot, C., and L. Margolis. 1991. Pacific salmon life histories. University of British Columbia Press, Vancouver, British Columbia, Canada.

Guill, C., B. Drossel, W. Just, and E. Carmack. 2011. A three-species model explaining cyclic dominance of Pacific salmon. Journal of Theoretical Biology 276:16–21.

Gurney, W. S. C., R. M. Nisbet, and J. H. Lawton. 1983. The systematic formulation of tractable single-species population models incorporating age structure. Journal of Animal Ecology 52:479–495.

Gustafson, R. G., T. C. Wainwright, G. A. Winans, F. W. Waknitz, L. T. Parker, and R. S. Waples. 1997. Status review of sockeye salmon from Washington and Oregon. NOAA Technical Memorandum NMFS-NWFSC-33.

Halley, J. M. 1996. Ecology, evolution, and 1/*f*-noise. Trends in Ecology and Evolution 11:33–37.

Hanski, I., H. Henttonen, E. Korpimäki, L. Oksanen, and P. Turchin. 2001. Small-rodent dynamics and predation. Ecology 82:1505–1520.

Heino, M., J. Ripa, and V. Kaitala. 2000. Extinction risk under colored environmental noise. Ecography 23:177–184.

Higgins, K., A. Hastings, J. N. Sarvela, and L. W. Botsford. 1997. Stochastic dynamics and deterministic skeletons: population behavior of Dungeness crab. Science 276:1431–1435.

Hilborn, R., T. P. Quinn, D. E. Schindler, and D. E. Rogers. 2003. Biocomplexity and fisheries sustainability. Proceedings of the National Academy of Sciences USA 100:6564–6568.

Holt, C. A., and R. M. Peterman. 2007. Long-term trends in age-specific recruitment of sockeye salmon (*Oncorhyncus nerka*) in a changing environment. Canadian Journal of Fisheries and Aquatic Sciences 61:2455–2470.

Krkosek, M., R. Hilborn, R. M. Peterman, and T. P. Quinn. 2011. Cycles, stochasticity and density-dependence in pink salmon population dynamics. Proceedings of the Royal Society B 278:2060–2068.

Larkin, P. A. 1971. Simulation studies of the Adams River sockeye salmon, *Oncorhyncus nerka*. Journal of the Fisheries Research Board of Canada 28:1493–1502.

Levy, D. A., and C. C. Wood. 1992. Review of proposed mechanisms for sockeye salmon cycles in the Fraser River. Bulletin of Mathematical Biology 54:241–261.

Martell, S. J. D., C. J. Walters, and R. Hilborn. 2008. Retrospective analysis of harvest management performance for Bristol Bay and Fraser River sockeye salmon (*Oncorhyncus nerka*). Canadian Journal of Fisheries and Aquatic Sciences 65:409–424.

May, R. M. 1973. Stability and complexity in model ecosystems. Princeton, University Press, Princeton, New Jersey, USA.

Moore, J. W., M. McClure, L. A. Rogers, and D. E. Schindler. 2010. Synchronization and portfolio performance of threatened salmon. Conservation Letters 3:340–348.

Mueter, F. J., B. J. Pyper, and R. M. Peterman. 2005. Relationships between coastal ocean conditions and survival rates of Northeast Pacific salmon at multiple lags. Transactions of the American Fisheries Society 134:105–119.

Murdoch, W. W. 1994. Population regulation in theory and practice. Ecology 75:271–287.

Murdoch, W. W., B. E. Kendall, R. M. Nisbet, C. J. Briggs, E. McCauley, and R. Bolser. 2002. Single species models for many-species food webs. Nature 417:542–543.

Myers, R. A., M. J. Bradford, J. M. Bridson, and G. Mertz. 1997. Estimating delayed density-dependent mortality in sockeye salmon (*Oncorhyncus nerka*): a meta-analytic approach. Canadian Journal of Fisheries and Aquatic Sciences 54:2449–2462.

Myers, R. A., G. Mertz, J. M. Bridson, and M. J. Bradford. 1998. Simple dynamics underlie sockey salmon (*Oncorhyncus nerka*) cycles. Canadian Journal of Fisheries and Aquatic Sciences 55:2355–2364.

Nisbet, R. 1997. Delay-differential equations for structured populations. Pages 89–118 *in* S. Tuljupurkar and H. Caswell, editors. Structured-population models in marine, terrestrial, and freshwater systems. Chapman and Hall, New York, New York, USA.

Peterman, R. M. 1981. Form of random variation in salmon smolt-to-adult relations and its influence on production estimates. Canadian Journal of Fisheries and Aquatic Sciences 38:1113–1119.

Peterman, R. M., and B. Dorner. 2011. Fraser River sockeye production dynamics. Cohen Commission Technical Report 10. Vancouver, British Columbia, Canada. http://www.cohencommission.ca/en/TechnicalReports.php

Peterman, R. M., and B. Dorner. 2012. A widespread decrease in productivity of sockeye salmon (*Oncorhyncus nerka*) populations in western North America. Canadian Journal of Fisheries and Aquatic Science 69:1255–1260.

Peterman, R. M., B. J. Pyper, M. F. Lapointe, M. D. Adkison, and C. J. Walters. 1998. Patterns of covariation in survival rates of British Columbian and Alaskan sockeye salmon (*Oncorhyncus nerka*) stocks. Canadian Journal of Fisheries and Aquatic Sciences 55:2503–2517.

Peterman, R. M., et al. 2010. Synthesis of evidence from a workshop on the decline of Fraser River sockeye. June 15–17, 2010. A Report to the Pacific Salmon Commission, Vancouver, British Columbia, Canada. http://www.cohencommission.ca/en/FinalReport/

Pyper, B. J., F. J. Mueter, and R. M. Peterman. 2005. Across-species comparisons of spatial scales of environmental effects on survival rates of Northeast Pacific salmon. Transactions of the American Fisheries Society 134:86–104.

Pyper, B. J., R. M. Peterman, M. F. Lapointe, and C. J. Walters. 1999. Patterns of covariation in length and age at maturity of British Columbia and Alaska sockeye salmon (*Oncorhyncus nerka*) stocks. Canadian Journal of Fisheries and Aquatic Sciences 56:1046–1057.

Ricker, W. E. 1950. Cycle dominance among the Fraser sockeye. Ecology 31:6–26.

Ricker, W. E. 1972. Hereditary and environmental factors affecting certain salmonid populations. Pages 19–160 *in* R. Simon and P. A. Larkin, editors. H. R. MacMillan lectures in fisheries. University of British Columbia, Vancouver, British Columbia, Canada.

Ricker, W. E. 1997. Cycles of abundance among Fraser River sockeye salmon (*Oncorhyncus nerka*). Canadian Journal of Fisheries and Aquatic Sciences 54:950–968.

Schindler, D. E., R. Hilborn, B. Chasco, C. P. Boatright, T. P. Quinn, L. A. Rogers, and M. S. Webster. 2010. Population diversity and the portfolio effect in an exploited species. Nature 465:609–613.

Schmitt, C. K., C. Guill, and B. Drossel. 2012. The robustness of cyclic dominance under random fluctuations. Journal of Theoretical Biology 308:79–87.

Sissenwine, M. P., and J. G. Shepherd. 1987. An alternative perspective on recruitment overfishing and biological reference points. Canadian Journal of Fisheries and Aquatic Sciences 65:765–779.

Sykes, Z. M. 1969. On discrete stable population theory. Biometrics 25:285–293.

Taylor, F. 1979. Convergence to the stable age distribution in populations of insects. American Naturalist 113:511–530.

Tilman, D., P. B. Reich, and J. H. M. Knops. 2006. Biodiversity and ecosystem stability in a decade-long grassland experiment. Nature 441:629–632.

Torrence, C., and G. P. Compo. 1998. A practical guide to wavelet analysis. Bulletin of the American Meteorological Society 79:61–78.

Turchin, P. 2003. Complex population dynamics: a theoretical/empirical synthesis. Princeton University Press, Princeton, New Jersey, USA.

Turchin, P., S. N. Wood, S. P. Ellner, B. E. Kendall, W. W. Murdoch, A. Fischlin, J. Casas, E. McCauley, and C. J. Briggs. 2003. Dynamical effects of plant quality and parasitism on population cycles of larch budmoth. Ecology 84:1207–1214.

Vasseur, D. A., and P. Yodzis. 2004. The color of environmental noise. Ecology 85:1146–1152.

Volterra, V. 1927. Variazioni e fluttuaioni del numero d'individui in specie animali conviventi. Regio Comitato Talassografico Italiano, Memoria 131:1–142.

Walters, C. J., and M. J. Staley. 1987. Evidence against the existence of cyclic dominance in Fraser River sockeye salmon (*Oncorhyncus nerka*). Canadian Special Publication in Fisheries and Aquatic Sciences 96:375–384.

Ward, F. J., and P. A. Larkin. 1964. Cyclic dominance in Adams River sockeye salmon. International Pacific Salmon Fisheries Commission Progress Report Number 11. New Westminster, British Columbia, Canada.

Worden, L., L. W. Botsford, A. Hastings, and M. D. Holland. 2010. Frequency responses of age-structured populations: Pacific salmon as an example. Theoretical Population Biology 78:239–249.

Supplemental Material

Appendix

Time series and wavelet spectra for sockeye salmon populations not shown in Fig. 1 (*Ecological Archives* M084-004-A1).

Supplement

MATLAB code used in simulations and analysis (*Ecological Archives* M084-004-S1).